containing P1198L with QuickChange™ site-directed mutagenesis system (Stratagene, La Jolla, CA, USA). The presence of P1198L and the absence of other mutations were confirmed by sequencing the whole insert.

COS-1 cells were plated on 35-mm dishes containing cover slips. The cells were then transiently transfected with wild-type or mutated human SUR1 cDNA (1.5 μg per dish) plus human Kir6.2 (1.5 μg per dish) using Lipofectamine 2000 (Invitrogen, Carlsbad, CA, USA). Recordings were made 24–72 h after transfection. The ATP sensitivity of the wild-type and mutant channels were determined basically as described previously[4,10] with a patch-clamp amplifier, Axopatch 200B (Axon Instruments, Foster City, CA, USA). Sulfonylurea sensitivity was assessed as the ratio between the amplitudes of the K_{ATP} channel currents before and after tolbutamide or glibenclamide application. Data were analyzed with pCLAMP (version 9.0; Axon Instruments), XLfit (CTC Laboratory System Corporation, Tokyo, Japan) and in-house software. Unpaired Student's *t*-test was used to test for statistical significances, and the results were expressed as mean ± SE.

RESULTS

Mutation Screening

We identified a heterozygous missense mutation in *ABCC8*. The mutation results in the substitution of leucine for proline at residue 1,198 in exon 29 (c.3593 C>T, p.P1198L, GenBank NM_000352). It was not found in the databases, such as dbSNP (http://www.ncbi.nlm.nih.gov/snp/) or 1,000 genome project (http://browser.1000genomes.org/index.html), and also in 150 unrelated Japanese subjects. The mutated residue is located within the short cytosolic loop that links transmembrane domains 15 and 16. The proline (P1198) is conserved across a range of species, from mammals (human and rat) to zebrafish, and is also found at a similar position in human SUR2. The *in silico* prediction programs, SIFT (http://sift.jcvi.org/) and PolyPhen-2 (http://genetics.bwh.harvard.edu/pph2/index.shtml), both predicted that the substitution would affect protein function. No mutations associated with diabetes were found in *KCNJ11* and *INS*.

Functional Analysis of Mutant K_{ATP} Channel

We tested the sensitivity of ATP to block the wild-type and the mutant K_{ATP} channels in inside-out membrane patches (Figure 2a). The concentration of ATP required to half-maximally inhibit the channel (IC_{50}) increased ≈ sevenfold from 23.4 ± 2.5 μmol/L for wild-type channels to 164.7 ± 19.3 μmol/L for mutant channels. This result shows that the mutant channel is less ATP sensitive than the wild type.

We next tested the response to sulfonylureas for the wild-type and the mutant K_{ATP} channels in inside-out membrane patches in nucleotide-free condition (Figure 2b). A total of 100 μmol/L tolbutamide inhibited the current by 65.6 ± 4.8% for the mutant channel, whereas 19.3 ± 5.2% for the wild type. In contrast, 30 nmol/L glibenclamide inhibited the current by 44.5 ± 6.5% for the mutant channel, whereas 10.8 ± 2.7% for the wild type. The residual current in the presence of

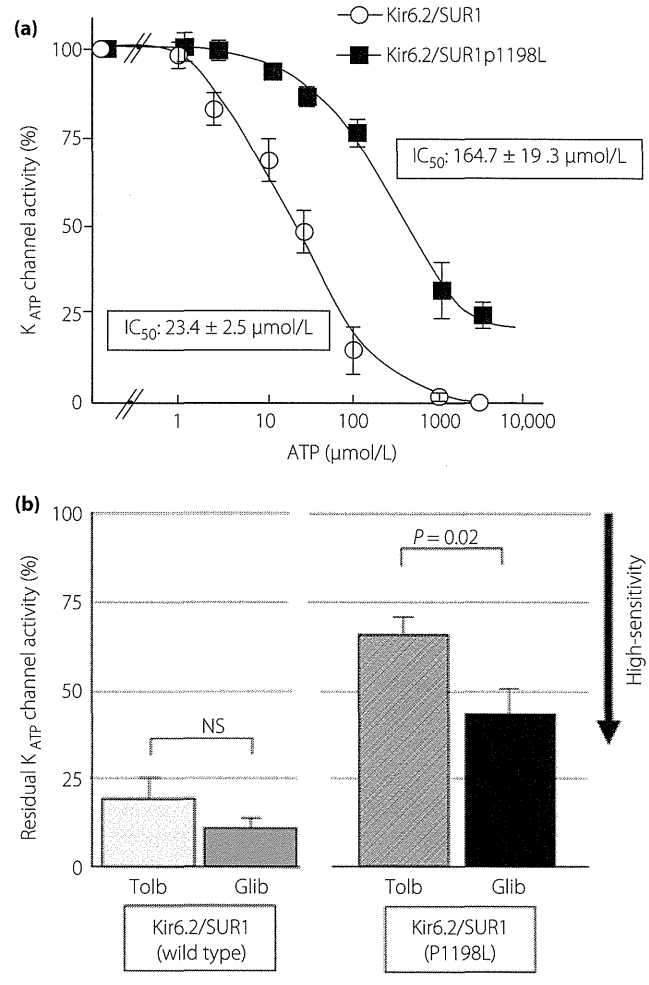

Figure 2 | (a) Adenosine triphosphate (ATP) sensitivity of wild-type and mutant ATP-sensitive potassium (K_{ATP}) channels. The dose-dependent inhibitory effects of ATP on the activities of the wild-type (Kir6.2/SUR1) and mutant (Kir6.2/SUR1P1198L) K_{ATP} channels are shown. Five experiments were carried out for each type of channel. The channel conductance of the mutant channel in a ATP-free condition was similar to that of the wild-type channel (73.1 ± 0.57 vs 72.9 ± 0.52 picosiemens (pS), P = 0.765). (b) Sulfonylurea sensitivity of the wild-type (Kir6.2/SUR1) or the mutant (Kir6.2/SUR1P1198L) K_{ATP} channels. Residual K_{ATP} channel activities were determined by the ratio between the amplitudes of K_{ATP} channel currents before and after 100 μmol/L tolbutamide (Tolb) or 30 nmol/L glibenclamide (Glib) applications. Data are mean ± standard error from seven independent experiments. IC_{50}, the concentration of adenosine triphosphate at which the inhibition is half of the maximal.

glibenclamide for the mutant channel was significantly smaller than that of tolbutamide (P = 0.02). These results show that the sensitivity to sulfonylureas is reduced in the mutant channel and glibenclamide is more effective than tolbutamide.

Clinical Effectiveness of Oral Sulfonylurea Therapy

After identification of an *ABCC8* gene mutation, the patient's treatment was switched from insulin injection (40 units a day)

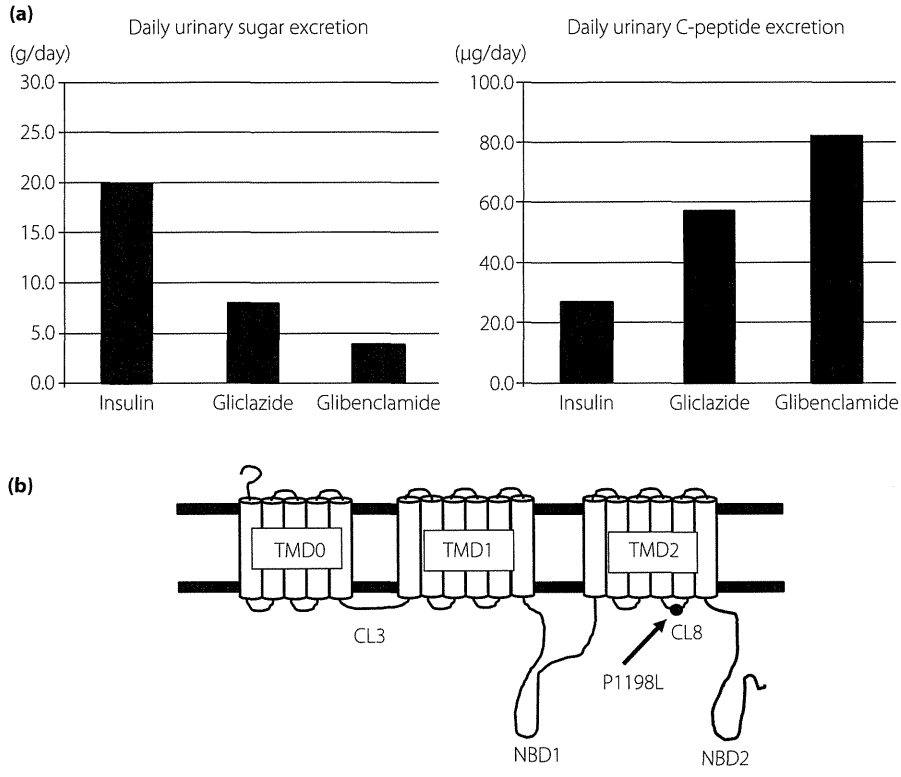

Figure 3 | (a) Daily urinary sugar excretion and daily urinary C-peptide excretion at insulin injection, high-dose gliclazide (a daily dose of 160 mg) or low-dose glibenclamide (a daily dose of 0.625 mg, which is 0.017 mg/kg/day) administration in the patient. (b) Schematic representation of the sulfonylurea receptor and the location of P1198L mutation (arrowed) identified in the patient. CL, cytosolic loop; NBD, nucleotide-binding domain; TMD, transmembrane domain.

to oral sulfonylureas under intensive monitoring in the hospital. Daily urinary C-peptide excretion, which was 27.8 μg/day before initiating sulfonylureas, increased to 58.1 μg/day at high-dose gliclazide (a daily dose of 160 mg) alone. Furthermore, daily urinary C-peptide excretion was further increased to 83 μg/day at low-dose glibenclamide (a daily dose of 0.625 mg, which is 0.017 mg/kg/day; Figure 3a). Simultaneously, daily urinary sugar excretion was decreased in inverse proportion to urinary C-peptide excretion (20.0, 8.0 and 4.0 g/day, respectively). Thus, oral glibenclamide treatment was selected for the patient's therapy and insulin injection was completely discontinued. Her blood glucose level was finally controlled with 0.17 mg/kg/day of glibenclamide.

DISCUSSION

In the present study, we identified the Pro1198Leu mutation in a patient with PNDM. The mutation was not found in the databases, such as dbSNP or 1,000 genome project, and also in 150 unrelated Japanese subjects. Furthermore, two *in silico* prediction programs, SIFT and PolyPhen-2, predicted that the mutation would affect protein function. We further confirmed that the mutant channel was less ATP sensitive than the wild type with a patch-clamp experiment. The degree of ATP insensitivity was comparable with that in a previous report for PNDM as a result of activating mutations in *ABCC8*[11]. These findings suggest that the P1198L mutation is strongly associated with the development of PNDM in the patient. Furthermore, it has only recently been reported from Turkey that the same mutation was identified in a girl with NDM[12]. In that report, the patient presented with severe hyperglycemia with ketoacidosis at 1 month-of-age and was initially treated with insulin. After genetic diagnosis, her treatment was successfully converted from insulin to glibenclamide (0.2 mg/kg/day). In addition, no neurological abnormality and no family history of diabetes were observed in the patient. These clinical characteristics were similar to the present case, except there was no family history of diabetes. In contrast, *in vitro* functional analysis of the mutation was not carried out in the report.

The mutated residue P1198 is located within the eighth cytosolic loop (CL8) that links transmembrane domains 15 and 16 in the SUR1 (Figure 3b). This loop has been reported to be a binding site of tolbutamide[13], and our functional analysis also showed that the sensitivity to tolbutamide was reduced in the mutant channel. Based on the drug structure, gliclazide is also thought to bind to the CL8. In contrast, in addition to the CL8, glibenclamide is able to bind to another site in the SUR1, which is located within the third cytosolic loop (CL3)[14]. This could explain the reason why glibenclamide was more effective both in patch-clamp experiments and in the patient.

In the family of the patient, her elder brother carried the P1198L mutation in the heterozygous state, whereas her mother did not (Figure 1). This suggests a possibility that her father might have the same mutation. The elder brother was diagnosed with diabetes at 11 years-of-age on medical examination at his school, but his diabetes was very mild and has been treated with diet alone. Furthermore, the proband's father, paternal aunt and paternal grandfather have diabetes. However, there is little information on these members, because her parents have divorced and members of her father's family did not agree to cooperate in the present study. The phenotypic variability of diabetes within families has been reported in some families with *ABCC8* gene mutations[8,15]. The precise reason for the variability is currently unknown. It might be explained by the influence of unknown other genetic and/or epigenetic factors.

Many patients with PNDM caused by *ABCC8* or *KCNJ11* gene mutations have been successfully treated with sulfonylureas[7,8]. In the present study, the treatment of our patient was also able to be switched from insulin injection to oral sulfonylurea therapy. In contrast, response to sulfonylureas has not been seen in PNDM caused by other gene mutations, such as *INS*[1]. This suggests that genetic diagnosis can provide clinical benefits to the patients with PNDM. It has been reported that genetic testing for *KCNJ11* and *ABCC8* in all children diagnosed before 6 months-of-age results not only in improved quality of life, but also in cost savings[16]. However, a large number of patients with PNDM have still been misdiagnosed as a very early onset form of type 1 diabetes and treated with insulin. The genetic diagnosis of PNDM will take on a growing importance in clinical practice.

ACKNOWLEDGEMENTS

The present study was supported by Scientific Research Grants from the Ministry of Education, Culture, Sports, Science and Technology of Japan, and from the Ministry of Health, Labor and Welfare of Japan. The authors declare no financial support or relationships that may pose a conflict of interest.

REFERENCES

1. Naylor RN, Greeley SA, Bell GI, *et al.* Genetics and pathophysiology of nenonatal diabetes mellitus. *J Diabetes Invest* 2011; 2: 158–169.
2. Suzuki S, Makita Y, Mukai T, *et al.* Molecular basis of neonatal diabetes in Japanese patients. *J Clin Endocrinol Metab* 2007; 92: 3979–3985.
3. Temple IK, Gardner RJ, Mackay DJ, *et al.* Transient neonatal diabetes: widening the understanding of the etiopathogenesis of diabetes. *Diabetes* 2000; 49: 1359–1366.
4. Inagaki N, Gonoi T, Clement JPT, *et al.* Reconstitution of IKATP: an inward rectifier subunit plus the sulfonylurea receptor. *Science* 1995; 270: 1166–1170.
5. Flanagan SE, Patch AM, Mackay DJ, *et al.* Mutations in ATP-sensitive K+ channel genes cause transient neonatal diabetes and permanent diabetes in childhood or adulthood. *Diabetes* 2007; 56: 1930–1937.
6. Edghill EL, Flanagan SE, Patch AM, *et al.* Insulin mutation screening in 1,044 patients with diabetes: mutations in the INS gene are a common cause of neonatal diabetes but a rare cause of diabetes diagnosed in childhood or adulthood. *Diabetes* 2008; 57: 1034–1042.
7. Pearson ER, Flechtner I, Njolstad PR, *et al.* Switching from insulin to oral sulfonylureas in patients with diabetes due to Kir6.2 mutations. *N Engl J Med* 2006; 355: 467–477.
8. Babenko AP, Polak M, Cave H, *et al.* Activating mutations in the *ABCC8* gene in neonatal diabetes mellitus. *N Engl J Med* 2006; 355: 456–466.
9. Kashiwagi A, Kasuga M, Araki E, *et al.* International clinical harmonization of glycated hemoglobin in Japan: from Japan Diabetes Society to National Glycohemoglobin Standardization program values. *J Diabetes Invest* 2012; 3: 39–40.
10. Beguin P, Nagashima K, Nishimura M, *et al.* PKA-mediated phosphorylation of the human K(ATP) channel: separate roles of Kir6.2 and SUR1 subunit phosphorylation. *EMBO J* 1999; 18: 4722–4732.
11. Ellard S, Flanagan SE, Girard CA, *et al.* Permanent neonatal diabetes caused by dominant, recessive, or compound heterozygous SUR1 mutations with opposite functional effects. *Am J Hum Genet* 2007; 81: 375–382.
12. Oztekin O, Durmaz E, Kalay S, *et al.* Successful sulfonylurea treatment of a neonate with neonatal diabetes mellitus due to a novel missense mutation, p.P1199L, in the *ABCC8* gene. *J Perinatol* 2012; 32: 645–647.
13. Ashfield R, Gribble FM, Ashcroft SJ, *et al.* Identification of the high-affinity tolbutamide site on the SUR1 subunit of the K(ATP) channel. *Diabetes* 1999; 48: 1341–1347.
14. Mikhailov MV, Mikhailova EA, Ashcroft SJ. Molecular structure of the glibenclamide binding site of the beta-cell K(ATP) channel. *FEBS Lett* 2001; 499: 154–160.
15. Patch AM, Flanagan SE, Boustred C, *et al.* Mutations in the *ABCC8* gene encoding the SUR1 subunit of the KATP channel cause transient neonatal diabetes, permanent neonatal diabetes or permanent diabetes diagnosed outside the neonatal period. *Diabetes Obes Metab* 2007; 9(Suppl 2): 28–39.
16. Greeley SA, John PM, Winn AN, *et al.* The cost-effectiveness of personalized genetic medicine: the case of genetic testing in neonatal diabetes. *Diabetes Care* 2011; 34: 622–627.

SUPPORTING INFORMATION

Additional Supporting Information may be found in the online version of this article:

Table S1 | Primer sequences for amplification of *ABCC8* gene

Clinical features of SCA36

A novel spinocerebellar ataxia with motor neuron involvement (Asidan)

Yoshio Ikeda, MD, PhD
Yasuyuki Ohta, MD, PhD
Hatasu Kobayashi, MD, PhD
Miyuki Okamoto, MD
Kazuhiro Takamatsu, MD
Taisei Ota, MD
Yasuhiro Manabe, MD, PhD
Koichi Okamoto, MD, PhD
Akio Koizumi, MD, PhD
Koji Abe, MD, PhD

Correspondence & reprint requests to Dr. Abe: ikeda006@cc.okayama-u.ac.jp

ABSTRACT

Objective: To characterize the phenotype of spinocerebellar ataxia type 36 (SCA36), a novel dominant disorder (nicknamed "Asidan") caused by a hexanucleotide GGCCTG repeat expansion in intron 1 of the *NOP56* gene.

Methods: We investigated the clinical, genetic, and neuropathologic characteristics of 18 patients with SCA36. We performed histologic evaluation of a muscle biopsy specimen from 1 patient with SCA36, and neuropathologic evaluation of an autopsied brain from another patient with SCA36.

Results: The (GGCCTG)n expansion was found in 18 ataxic patients from 9 families. The age at onset of ataxia was 53.1 ± 3.4 years, with the most frequent symptoms being truncal ataxia (100% of patients), ataxic dysarthria (100%), limb ataxia (93%), and hyperreflexia (79%). Tongue fasciculation and subsequent atrophy were found in 71% of cases, particularly in those of long duration. Skeletal muscle fasciculation and atrophy of the limbs and trunk were found in 57% of cases. Lower motor involvement was confirmed by EMG and muscle biopsy. The neuropathologic study revealed significant cerebellar Purkinje cell degeneration with obvious loss of lower motor neurons. Immunohistochemical analysis showed that NOP56 was localized to the nuclei of various neurons. Cytoplasmic or intranuclear inclusion staining of NOP56, TDP-43, and ataxin-2 was not observed in the remaining neurons.

Conclusions: This is the first description of the unique clinical features of SCA36, a relatively pure cerebellar ataxia with progressive motor neuron involvement. Thus, SCA36 is a disease that stands at the crossroads of SCA and motor neuron disease. *Neurology*® 2012;79:333-341

GLOSSARY

ALS = amyotrophic lateral sclerosis; **CMAP** = compound muscle action potential; **eZIS** = easy Z-score imaging system; **H&E** = hematoxylin & eosin; **MCP** = middle cerebellar peduncle; **MCV** = motor nerve conduction velocity; **NADH-TR** = *nicotinamide adenine dinucleotide-tetrazolium reductase*; **NCS** = *nerve conduction study*; **SARA** = *Scale for Assessment and Rating of Ataxia*; **SCA** = spinocerebellar ataxia; **SCV** = sensory nerve conduction velocity; **SNAP** = sensory nerve action potential; **^{99m}Tc-ECD** = ^{99m}Tc-ethylcysteinate dimer.

Dominantly inherited spinocerebellar ataxias (SCAs) are a heterogeneous group of neurodegenerative disorders. More than 30 different loci involving 22 genes have been reported for the SCA subtypes.[1] Identification of the genes responsible for the SCA subtypes will help clarify the molecular pathomechanism leading to cerebellar degeneration and ataxia. However, the increasing number of SCAs adds to the clinical heterogeneity, and detailed characterization of the disease phenotypes will be needed to understand the natural history of the disease and to provide appropriate medical or genetic counseling to affected patients.

Here, we report the clinical, genetic, and neuropathologic characteristics of a novel type of SCA, SCA36, which we recently identified as being due to a hexanucleotide GGCCTG repeat expansion in intron 1 of the nucleolar protein 56 (*NOP56*) gene.[2] SCA36 frequently displays unique clinical

Editorial, page 302

From the Department of Neurology (Y.I., Y.O., M.O., K.T., T.O., K.A.), Graduate School of Medicine, Dentistry and Pharmaceutical Sciences, Okayama University, Okayama; Department of Health and Environmental Sciences (H.K., A.K.), Graduate School of Medicine, Kyoto University, Kyoto; Department of Neurology (M.O., K.T., T.O.), Ota Memorial Hospital, Fukuyama; Department of Neurology (Y.M.), National Hospital Organization Okayama Medical Center, Okayama; and Department of Neurology (K.O.), Gunma University Graduate School of Medicine, Maebashi, Japan.

Study funding: Supported in part by Grants-in-Aid for Scientific Research (C) 21591084 (to Y.I.) and Scientific Research (B) 21390267 (to K.A.) from the Ministry of Education, Culture, Sports, Science and Technology, Japan, and by Grants-in-Aid from the Research Committees (Nakano I, Sobue G, Mizusawa H, Nishizawa M, and Sasaki H), the Ministry of Health, Labour and Welfare, Japan (to K.A.).

Go to Neurology.org for full disclosures. Disclosures deemed relevant by the authors, if any, are provided at the end of this article.

features involving motor neurons characteristically found in the tongue and limbs. The clinical course of SCA36, which we have named "Asidan," typically progresses slowly and functional ability, including swallowing, is generally well-preserved even at an advanced stage. The multiple system involvement of SCA36 indicates that the (GGCCTG)n expansion may affect the biological pathways that bridge degenerative ataxia and motor neuron disease.

METHODS

Subjects and clinical examination. We recruited patients with dominantly inherited ataxia who visited our clinic. All subjects gave a clinical history and underwent a clinical examination and evaluation, including the Scale for Assessment and Rating of Ataxia (SARA).

Standard protocol approvals, registrations, and patient consents. Ethical approval for the clinical and genetic evaluation of ataxia families was obtained from the local ethics committee of Okayama University. All participants gave written informed consent for this study.

Genetic analysis. Genomic DNA was extracted from peripheral blood leukocytes of subjects in the dominant ataxia families. DNA was screened for the CAG triplet expansions present in SCA types 1–3, 6–8, and DRPLA, and for insertion of the long pentanucleotide (TGGAA)n repeat present in SCA31, using previously described methods.[3,4] A genetic diagnosis of SCA36 was confirmed by the presence of a (GGCCTG)n repeat expansion in the *NOP56* gene, either by Southern blot analysis or repeat-primed PCR analysis, according to our previous report.[2]

Electrophysiologic study. Peripheral nerve conduction studies (NCSs) and EMG were performed on 11 affected individuals from 8 families, and 2 affected individuals from 2 families. NCSs and EMGs were measured with an NCS/EMG recording system (Neuropack; Nihon Koden, Tokyo, Japan) using conventional procedures. Measurements were made of motor and sensory nerve conduction velocities (MCV/SCV), amplitude of compound muscle action potential (CMAP) or sensory nerve action potential (SNAP), and distal latencies of each nerve.

Muscle biopsy. The muscle biopsy was taken from the left biceps brachii muscle of patient II-4 in pedigree G (figure 1), whose disease was complicated by general muscle atrophy. The biopsy specimen was rapidly frozen, and 10-μm sections were prepared horizontally against the muscle fibers. Sections were visualized by staining with hematoxylin & eosin (H&E), nicotinamide adenine dinucleotide-tetrazolium reductase (NADH-TR), and Gomori trichrome, using conventional procedures.

Neuroimaging study. A 1.5-T brain MRI or CT scan was performed on 14 affected individuals from 9 families. Sagittal, coronal, and horizontal sections of MRI scans were evaluated to detect sites of degeneration. SPECT with ^{99m}Tc-ethylcysteinate dimer (^{99m}Tc-ECD) was performed in 11 affected individuals, and statistical imaging analysis was performed with the easy Z-score imaging system (eZIS).[5]

Neuropathology. A neuropathologic examination was performed on the brain and upper cervical cord of the affected individual II-4 in pedigree E (figure 1); this individual died at age 86. Paraffin-embedded sections of 4.5-μm thickness were visualized by H&E staining. Immunohistochemical staining was performed with antibodies against NOP56 (sc-133839, Santa Cruz Biotechnology, Santa Cruz, CA), TDP-43 (10782-2-AP, ProteinTech, Chicago, IL), ataxin-2 (HPA020339, Sigma, St. Louis, MO), and β-amyloid (SIG-39220, Covance, Princeton, NJ). Positive staining was visualized using the avidin-biotin-peroxidase complex method with diaminobenzidine as the chromogen (Vector Laboratories, CA). Negative control sections were processed in the same manner but with the primary antibody omitted. For enumeration of neurons, digital images of H&E-stained microscopic sections were analyzed with ImageJ 1.44 software (NIH, Bethesda, MD). The number of Purkinje cells per 1 mm in the external granule cell layer at the upper part of the vermis, and the number of cerebellar dentate neurons per 1 mm^2, were counted on 10 microscopic fields (100× magnification) of tissues from the patient with SCA36 and 3 healthy controls (who died at age 85 or 86). The number of hypoglossal and spinal motor neurons at both sides were counted on 3 sections each from the patient with SCA36 and the healthy controls.

RESULTS

Clinical characteristics of affected individuals with the SCA36 mutation. We identified a total of 18 ataxia patients from 9 families with a (GGCCTG)n repeat expansion in the *NOP56* gene. The pedigrees of these families are shown in figure 1, which shows the autosomal dominant transmission of the ataxic phenotype. All 8 unaffected family members genetically at risk for the disease did not have the (GGCCTG)n repeat expansion, indicating a disease penetrance of nearly 100%. From the 9 families, 14 affected individuals were clinically evaluated in detail. The mean age at onset of the disease was 53.1 ± 3.4 years (mean ± SD; range 47–58 years), with truncal ataxia as the most frequent initial symptom. The mean age at examination was 67.1 years and the mean duration of the illness was 13.9 years. All affected patients showed cerebellar ataxia, and in most cases, the severity of the symptoms was in the following order: truncal ataxia, ataxic dysarthria, limb ataxia, and dysdiadochokinesis (table). Other frequently observed features included hyperreflexia (79%) in the upper and lower limbs, with increased muscle tone in 29% of the patients. However, no patients showed pathologic reflexes such as the extensor plantar response. Impaired smooth pursuit and horizontal gaze nystagmus were found in 93% and 29%, respectively. Tongue atrophy or fasciculation was found in 10 cases (71%). Dysphagia was observed but did not impair oral intake for at least 10 years after disease onset. Tongue fasciculation was characteristically seen at the lateral edge, and was more evident on protrusion of the tongue. Tongue atrophy was found in all patients with disease duration longer than 10 years. The tongue atrophy found in patient II-4 in pedigree G is shown in figure 2A. Skeletal muscle atrophy in the limbs and trunk was found in 9 cases (64%), with fasciculation present in 8 cases (57%).

Figure 1 **Pedigrees of 9 families with spinocerebellar ataxia type 36 (SCA36)**

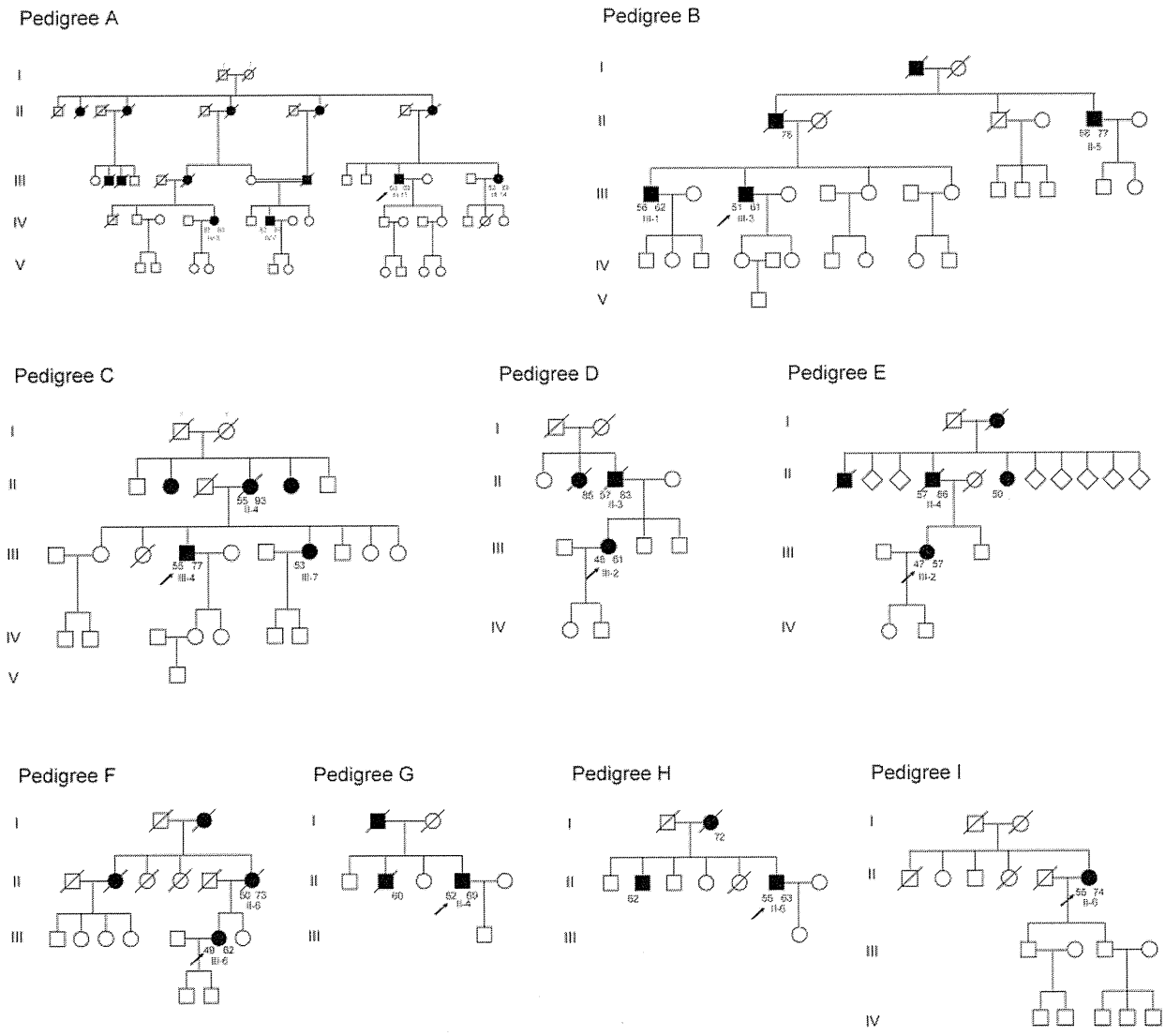

Pedigrees A to I are the SCA36 families evaluated in this study. Affected individuals are shown with filled symbols, and diagonal lines denote deceased individuals. Squares and circles represent males and females, respectively. The proband is indicated by an arrow. The number at the lower left corner is the age at onset, and the number at the lower right corner is the current age or the age at death.

Muscle atrophy and weakness were observed predominantly in the distal part of limbs. Muscle tone was generally normal, but a few cases showed increased or decreased tone depending on the balance between upper and lower motor neuron involvements. Superficial and deep sensory disturbance, parkinsonism, and urinary disturbance were not found. The total SARA scores ranged from 9.0 to 34.0 points with the greatest impairment seen for truncal stability. No patients complained of depression or other mood disorders. Serum creatine kinase levels were normal (35–112 IU/L). Analysis of 5 transmissions from 4 pedigrees showed a difference in age at onset for the older vs the younger generations of between −10 and 0 years, with an average of −4.4 years. Within these 5 parent-offspring pairs, there was no evidence of accelerated progression of the disease symptoms, and anticipation of age at onset was not confirmed in either paternal or maternal transmission.

Genetic analysis of dominant ataxia families. We found 10 families with dominant ataxia in an area along the river Asida, located in the western part of the main island of Japan. The families carried none of the known SCA mutations. In a previous report, we described a genome-wide linkage study of 3 of the 10 Asida River families (pedigrees A, B, and C in figure 1) for which multiple family members were available for analysis. That study identified association with a single genetic locus on chromosome 20p13, and subsequently, a hexanucleotide (GGCCTG)n repeat expansion in the *NOP56* gene was found as the mutation responsible for

Table **Clinical features of affected individuals in 9 families with SCA36**

	Pedigree A			Pedigree B			Pedigree C	Pedigree D	Pedigree E		Pedigree F	Pedigree G	Pedigree H	Pedigree I
	III-14	IV-5	IV-7	II-5	III-1	III-3	III-4	III-2	II-4	III-2	III-6	II-4	II-6	II-6
Gender	F	F	M	M	M	M	M	F	M	F	F	M	M	F
Age at onset, y	52	57	52	58	56	51	55	48	57	47	49	52	55	55
Age at examination, y	68	63	59	77	62	61	77	61	86	57	62	69	63	74
Duration of illness, y	16	6	7	19	6	10	21	13	29	10	13	17	8	19
Truncal ataxia	3+	2+	+	3+	2+	3+	3+	2+	3+	3+	3+	3+	2+	3+
Ataxic dysarthria	2+	+	+	2+	+	2+	2+	+	3+	2+	2+	3+	2+	3+
Limb ataxia	3+	+	+	2+	±	+	2+	+	3+	+	+	2+	2+	2+
Gaze nystagmus	+	+	–	+	–	–	+	–	–	–	–	–	–	–
Tongue atrophy	+	+	+	+	±	+	+	2+	+	+	+	3+	2+	3+
Tongue fasciculation	±	+	±	+	±	+	+	2+	–	2+	+	3+	+	+
Dysphagia	2+	±	–	–	–	+	–	2+	3+	–	±	2+	–	+
Muscle atrophy (limbs and trunk)	+	–	–	2+	–	+	2+	+	3+	+	–	3+	–	+
Muscle fasciculation (limbs and trunk)	+	–	–	+	–	+	+	±	+	+	–	3+	–	+
Muscle weakness	+	–	–	–	–	–	–	2+	2+	–	–	3+	–	+
Increased muscle tone	–	–	–	–	–	+	–	+/LE	–	–	+/LE	+/LE	–	–
Decreased muscle tone	–	–	–	+	–	–	–	+/UE	–	–	–	+/UE	–	+
Jaw reflex	–	–	–	–	–	–	–	–	–	–	±	–	–	+
Biceps brachii reflex[a]	2+/2+	2+/2+	2+/2+	+/+	2+/2+	2+/2+	2+/2+	2+/2+	+/+	2+/2+	3+/3+	3+/3+	+/+	3+/3+
Triceps brachii reflex[a]	2+/2+	+/+	+/+	+/+	2+/2+	2+/2+	2+/2+	2+/2+	+/+	2+/2+	3+/3+	3+/3+	+/+	3+/3+
Patellar tendon reflex[a]	3+/3+	2+/2+	2+/2+	+/+	2+/2+	2+/2+	2+/2+	2+/2+	+/+	2+/2+	3+/3+	3+/3+	+/+	3+/3+
Achilles tendon reflex[a]	±/+	+/+	+/+	–/–	+/+	+/+	+/+	3+/3+	–/–	+/+	3+/3+	3+/3+	+/+	3+/3+
Extensor plantar response (Babinski)[a]	–/–	–/–	–/–	–/–	–/–	–/–	–/–	–/–	–/–	–/–	–/–	–/–	–/–	–/–
Reduced vibratory sense	–	–	–	–	–	–	–	–	–	–	–	–	–	–
SARA score	25.5	13.0	9.0	25.0	14.0	24.0	26.0	21.0	NE	14.0	22.0	34.0	20.5	NE
Atrophy on brain MRI/CT	Cbl	Cbl	Cbl	Cbr, Cbl	Cbl	Cbl	Cbl	Cbl	Cbr, Cbl	Cbl	Cbl	Cbl	Cbl	Cbl

Abbreviations: – = symptom absent; ± = symptom subtle; + = symptom mild; 2+ = symptom moderate; 3+ = symptom severe; Cbl = cerebellum; Cbr = cerebrum; LE = lower extremities; NE = not examined; SARA = Scale for Assessment and Rating of Ataxia; SCA = spinocerebellar ataxia; UE = upper extremities.
[a] Reflex scores are given for right/left sides.

the disease.[2] In total, 9 Asida River families in our cohort carried this novel repeat expansion, as confirmed by Southern blot analysis and repeat-primed PCR analysis (pedigrees A through I in figure 1). The number of GGCCTG repeats in the expansions in 17 affected individuals was estimated by Southern blot analysis to range from 1,700 to 2,300.[2] The number of expanded repeats did not correlate with the age at onset or the SARA score, i.e., affected individuals with longer (GGCCTG)n repeats did not show earlier age at onset or more severe ataxia.[2]

Electrophysiologic findings in affected individuals. The mean values for the MCV/SCV, CMAP/SNAP amplitudes, and their distal latencies in the median, ulnar, tibial, peroneal, and sural nerves were all within normal ranges. The EMG studies demonstrated the fibrillation and fasciculation potentials and increased insertional activities recorded at multiple sites of limb and truncal muscles. The motor unit potentials showed high amplitude (up to 8.0 mV) and long duration (over 10 msec). The EMG with maximum muscle contraction showed a discrete interference pattern. Examples of the EMG recordings from patient II-4 in pedigree G are shown in figure 2B.

Histologic findings from muscle biopsy. H&E staining of the biopsy from one affected patient revealed grouped atrophy of the muscle fibers, small angular muscle fibers, and pyknotic nuclear clumps (figure 2C). The NADH-TR staining showed fiber-type grouping

Figure 2 **Clinical and laboratory findings of a patient with spinocerebellar ataxia type 36**

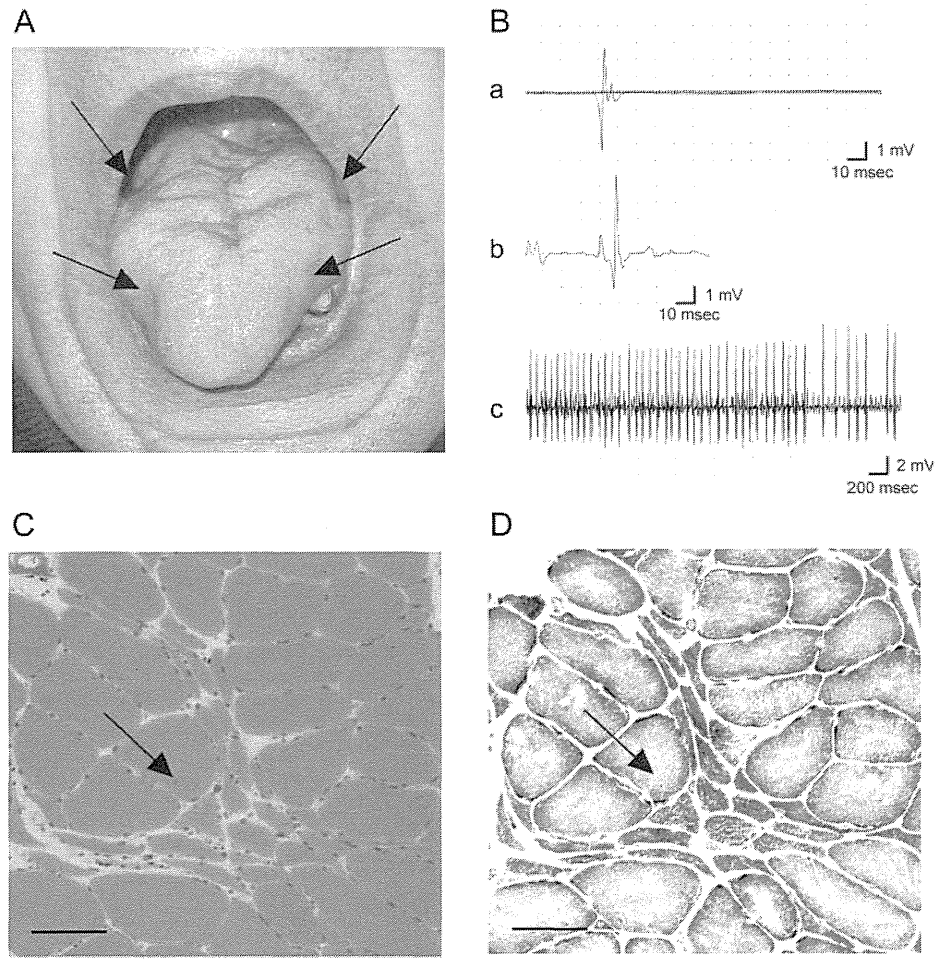

(A) An example of typical tongue atrophy found in II-4 in pedigree G. Arrows indicate the sites of prominent atrophy. (B) Examples of the EMG recordings examined in II-4 in pedigree G. A fasciculation potential recorded at the left pectoralis major muscle at rest (a), and the neurogenic EMG findings recorded at the right biceps brachii muscle with minimum and maximum contraction (b and c, respectively) are shown. (C) Photomicrographs of the muscle biopsy from the left biceps brachii muscle from patient II-4 in pedigree G. Hematoxylin & eosin staining revealed grouped atrophy of muscle fibers, small angular muscle fibers, and pyknotic nuclear clumps (arrow). Scale bar = 100 μm. (D) Nicotinamide adenine dinucleotide-tetrazolium reductase staining showed fiber-type grouping of darkly stained atrophic muscle fibers (arrow). Scale bar = 100 μm.

of darkly stained atrophic muscle fibers (figure 2D). The Gomori trichrome staining did not show ragged-red muscle fibers. There were no centrally located nuclei in muscle fibers, and no evidence of inflammation. These findings indicated that the patient had neurogenic muscle atrophy with chronic denervation.

Neuroimaging findings. The brain MRI of 13 affected individuals, and the brain CT of 1 affected individual, showed prominent atrophy of the cerebellar vermis and hemispheres, and dilation of the fourth ventricle. In most cases, the middle cerebellar peduncles (MCPs), brainstem, and cerebral hemispheres were relatively preserved. Representative MRI scans of the affected individual IV-5 in pedigree A are shown in figure 3, Aa–Ac. Abnormal intensities in the cerebellar and cerebral parenchyma were not seen. The affected individuals with disease duration between 17 and 29 years (III-4 in pedigree C; figure 3, Ba–Bc, and II-4 in pedigree E; figure 3Cc, respectively) showed minimal atrophy of the pons and MCPs, and other patients showed no pontine atrophy. The brain CT scans of the affected individual II-4 in pedigree E also showed bilateral frontal lobe atrophy, but no obvious abnormal densities in the cerebral parenchyma (figure 3, Ca and Cb). This patient had long been bedridden due to complicating diseases and also had dementia (figure 3Cd), however, his neuropsychological deficits could not be evaluated because of limited communication at the time we examined. The eZIS statistical imaging analysis of the ^{99m}Tc-ECD SPECT examined in 11 affected individuals revealed hypoperfusion in the cerebellar vermis and hemispheres, as shown in figure 3Ad. Individual III-4 in pedigree C had long disease

Figure 3 **Neuroradiologic findings of patients with spinocerebellar ataxia type 36**

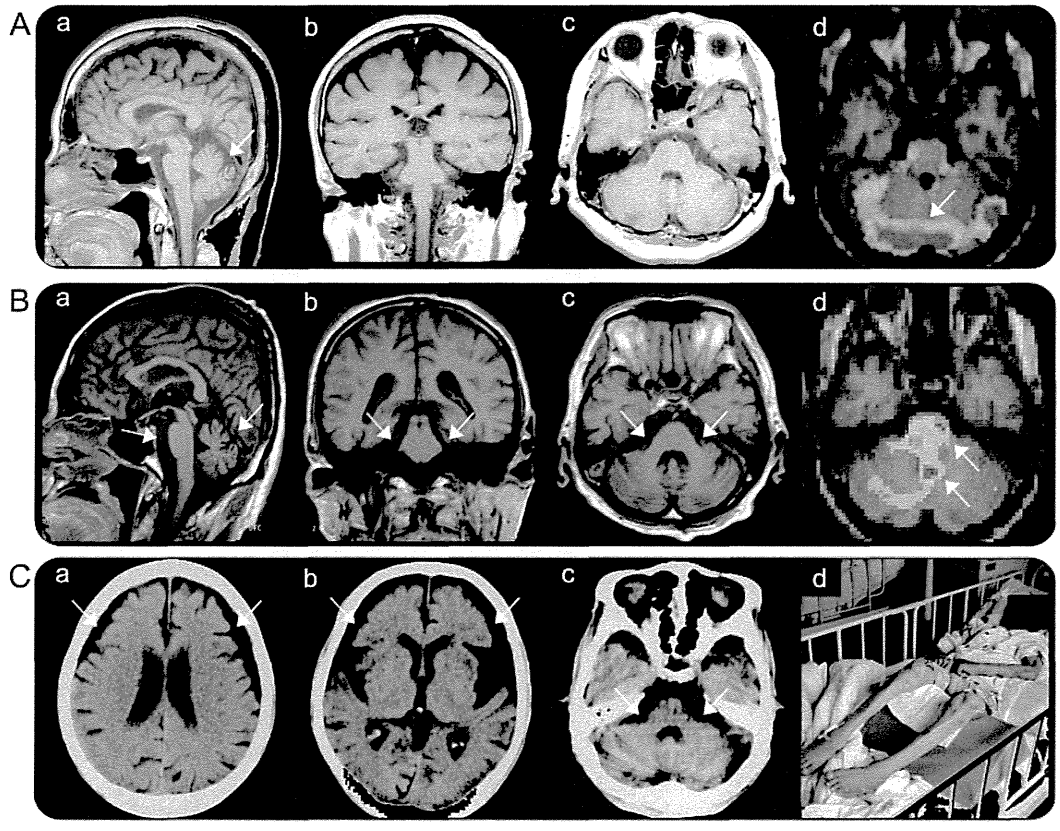

(A) MRI scans of an affected individual IV-5 in pedigree A with disease of 6 years duration. Midsagittal, coronal, and horizontal sections are shown (Aa, Ab, Ac, respectively). Arrow in (Aa) indicates atrophy of the upper part of cerebellar vermis. The pons and middle cerebellar peduncles (MCPs) are relatively preserved (Ab and Ac). The easy Z-score imaging system (eZIS) statistical imaging analysis of the ^{99m}Tc-ethylcysteinate dimer (^{99m}Tc-ECD) SPECT shows hypoperfusion in the cerebellar vermis and hemispheres (Ad, arrow). (B) MRI scans of an affected individual III-4 in pedigree C with disease of 21 years duration. Midsagittal, coronal, and horizontal sections are shown (Ba, Bb, Bc, respectively). Arrows in (Ba) indicate mild atrophy of pons and severe atrophy of cerebellar vermis. Arrows in (Bb) and (Bc) indicate atrophy of MCPs. The eZIS statistical imaging analysis of the ^{99m}Tc-ECD SPECT showed hypoperfusion in both the cerebellum and pons (Bd, arrows). (C) Brain CT scans of an affected individual II-4 in pedigree E with disease of 29 years duration. Scans show bilateral frontal lobe atrophy (arrows in Ca and Cb) combined with pontine and cerebellar atrophy (arrows in Cc). This patient had long been bedridden due to complicating diseases (Cd).

duration and exhibited hypoperfusion in both the cerebellum and pons, but not in the midbrain or other parts of the brain (figure 3Bd).

Neuropathologic findings. The brain of individual II-4 in pedigree E was analyzed in detail. The total brain weight including the cerebellum and brainstem was 990 g, and the cerebellum weight was 90 g. Macroscopically, the cerebellum and the cerebrum showed moderate atrophy, which was most pronounced in the frontal region of the cerebrum and the vermis of the cerebellum. The brainstem was relatively preserved.

In comparison to a healthy control (figure 4, Aa–Ae), microscopic analysis of the patient with SCA36 showed pronounced neuronal loss in the Purkinje cell layer of the cerebellum (figure 4, Af and Ag) and in the dentate nuclei (figure 4Ah). No overt neuronal loss was observed within the pontine and inferior olivary nuclei. In addition to the cerebellar degeneration, the patient brain showed loss of motor neurons in the hypoglossal nucleus (figure 4Ai) and the anterior horn at the upper cervical cord (figure 4Aj). Enumeration of the microscopic findings showed there were fewer Purkinje cells (figure 4Ba) and cerebellar dentate neurons (figure 4Bb) in the SCA36 cerebellum than in the healthy controls. Similarly, there were fewer motor neurons at the hypoglossal nucleus or the anterior horn in the patient with SCA36 than in the healthy controls (figure 4Bc). It should also be noted that we did not observe any neurons with Bunina bodies or other cytoplasmic inclusions associated with amyotrophic lateral sclerosis (ALS) pathology. β-Amyloid-positive plaques were not observed in the frontal cortex of the patient with SCA36.

Immunohistochemical analysis showed NOP56 staining localized in the nuclei of various neurons,

Figure 4 Neuropathologic findings of a patient with spinocerebellar ataxia type 36 (SCA36)

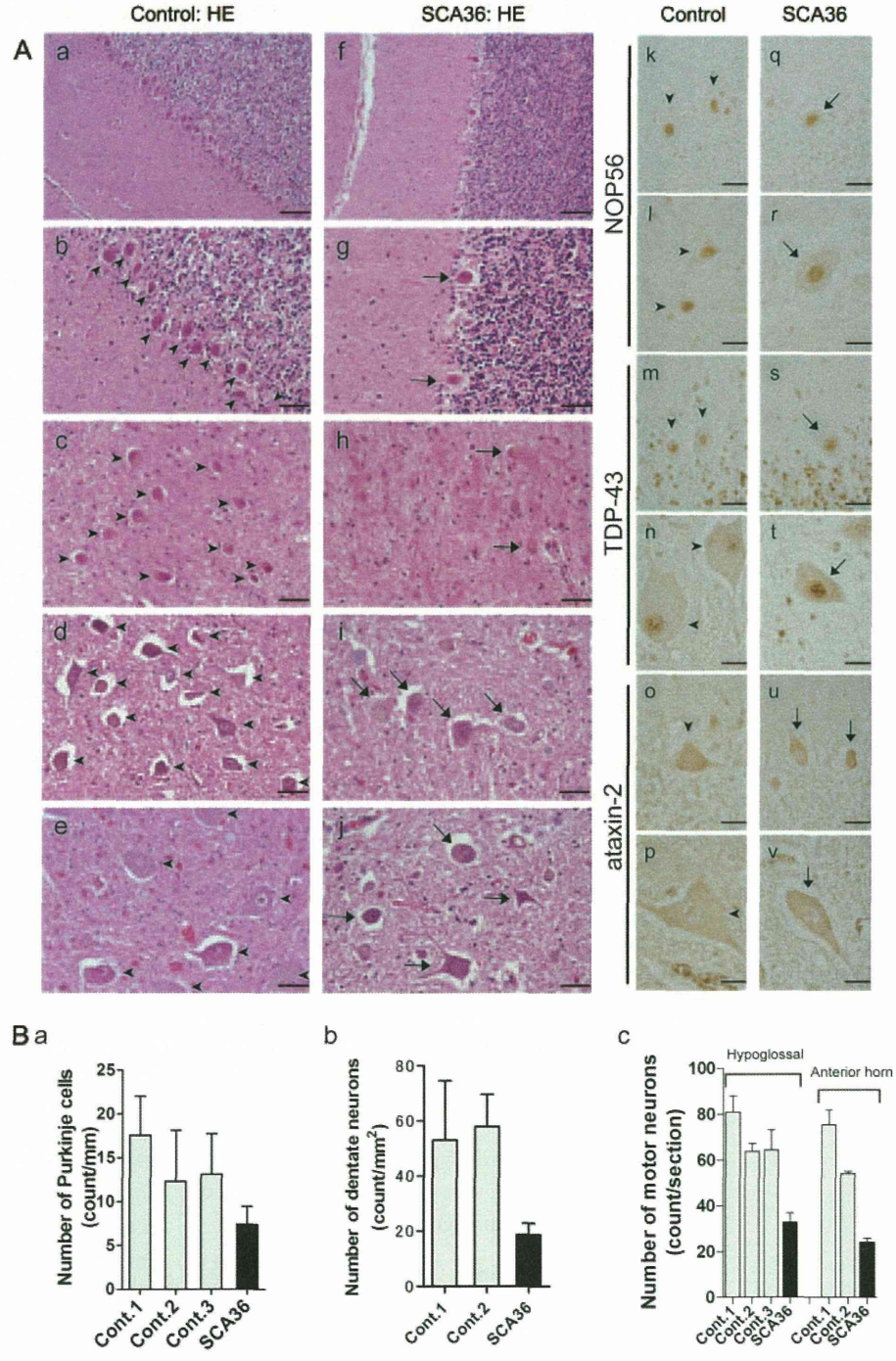

(A) Photomicrographs of hematoxylin & eosin-stained brain and spinal cord sections from a healthy control subject and a patient with SCA36 (II-4 in pedigree E) are shown in the left (a–e) and the middle (f–j) columns, respectively. Hematoxylin & eosin staining revealed pronounced neuronal loss in the Purkinje cell layer of the cerebellum (f and g) and in the dentate nuclei (h) of the patient with SCA36. Loss of motor neurons in the hypoglossal nucleus (i) or the anterior horn at the upper cervical cord (j) was confirmed without Bunina bodies or other cytoplasmic inclusions in the remaining neurons. NOP56 immunohistochemistry showed localization in the nuclei of the cerebellar Purkinje cells (k and q) and the spinal motor neurons (l and r) in both the healthy control (k and l) and the patient with SCA36 (q and r). The TDP-43 immunohistochemistry showed nuclear localization in neurons including the cerebellar Purkinje cells (m and s) and the spinal motor neurons (n and t). The ataxin-2 immunohistochemistry showed cytoplasmic localization in neurons including the cerebellar Purkinje cells (o and u) and the spinal motor neurons (p and v). The location of neurons in sections from the healthy control and the patient with SCA36 is indicated by an arrowhead (b–e and k–p) and an arrow (g–j and q–v), respectively. Scale bar = 100 μm (a and f), 50 μm (b–e and g–j), and 25 μm (k–v). (B) Quantitative analysis of the number of Purkinje cells (a), cerebellar dentate neurons (b), and motor neurons at the hypoglossal nucleus or the spinal anterior horn (c), in the patient with SCA36 and healthy controls.

including the cerebellar Purkinje cells (figure 4, Ak and Aq) and the spinal motor neurons (figure 4, Al and Ar). NOP56 immunoreactivity in these neurons was comparable in the healthy control (figure 4, Ak and Al) and the patient with SCA36 (figure 4, Aq and Ar). No NOP56-positive intranuclear inclusions or focal accumulations were detected in the patient with SCA36 (figure 4, Aq and Ar).

Immunohistochemical staining showed TDP-43 to be localized to the nucleus in the cerebellar Purkinje cells (figure 4, Am and As) and the spinal motor neurons (figure 4, An and At). There was no evidence of TDP-43 mislocalization in the cytoplasm, intracellular inclusions, or focal accumulations in the patient with SCA36 (figure 4, As and At).

The ataxin-2 immunohistochemical staining showed cytoplasmic localization in neurons, including the cerebellar Purkinje cells (figure 4, Ao and Au) and the spinal motor neurons (figure 4, Ap and Av). No ataxin-2-positive intracellular inclusions or focal accumulations were detected in the patient with SCA36 (figure 4, Au and Av).

DISCUSSION The affected individuals in the Asida River families displayed uniform clinical features, suggesting that the gene defect in these families may be transmitted from a common founder (figure 1 and table). As expected, our linkage study identified a single locus on chromosome 20p13, where the locus for SCA23 in a single Dutch family had also been mapped.[2,6,7] The mutation responsible for SCA23 was recently identified in the prodynorphin (*PDTN*) gene.[8] In addition, the defect in a Chinese family with dominant ataxia was mapped to the same locus as SCA23 and was identified as a missense mutation in the transglutaminase 6 (*TGM6*) gene (SCA35).[9] Although they are all located in the same region, we showed that the mutation in the Asida River families is located in a separate gene to those responsible for SCA23 and SCA35; the (GGCCTG)n repeat expansion lies in the *NOP56* gene (SCA36).[2] This novel type of repeat expansion was found in 9 families in our cohort (figure 1). All 9 families shared a common affected haplotype, supporting the likelihood of a founder effect in these families.[2] In our previous study, we saw no significant difference in *NOP56* RNA or protein expression between SCA36 and control lymphoblasts, and "RNA foci" containing aggregates of expanded GGCCUG transcripts were found in the nuclei of SCA36 lymphoblasts, suggesting a likely RNA gain-of-function mechanism in the pathogenesis of SCA36.[2]

In the current study, neurologic examinations of the SCA36 families characterized this disorder as slowly progressive cerebellar ataxia with involvement of upper and lower motor neurons (table), features that are distinct from other forms of dominant SCA. Surprisingly, tongue atrophy or fasciculation was found in 10 of 14 cases (71%, table). Tongue atrophy was commonly found in cases of longer than 10 years duration, and fasciculation became more evident when the tongue was protruded (figure 2A).[10] Skeletal muscle atrophy or fasciculation in limbs and trunk was found in 8 cases (57%); however, some patients were wheelchair-bound due to progression of ataxia rather than limb weakness. In agreement with the normal NCS findings, no patients had peripheral neuropathy. The neurogenic EMG findings (figure 2B) and the presence of neurogenic muscle atrophy confirmed by muscle biopsy (figure 2, C and D) support the lower motor neuron involvement in the pathogenesis of SCA36.

The neuropathologic studies of the patient with SCA36 revealed cerebellar degeneration combined with loss of motor neurons in the hypoglossal nucleus and the spinal anterior horn, which may explain the neurologic findings and impairment in patients with SCA36. Importantly, we failed to detect several findings characteristic of ALS. No cytoplasmic or intranuclear inclusions were identified in the neurons by H&E staining, or by NOP56, TDP-43, and ataxin-2 immunohistochemistry. Mislocalization of nuclear TDP-43 in the cytoplasm and distinct cytoplasmic ataxin-2 accumulation, which have been reported in the neuropathology of ALS cases, were not observed.[11,12]

SCA36 exhibits clinical similarities and differences to SCA23 and SCA35, which map to the same chromosomal region.[6,7,9] The age at onset in SCA36 (53.1 years) is similar to that in SCA23 (50.4 years) but is much less in SCA35 (43.7 years). The high frequency of hyperreflexia found in patients with SCA36 (79%) was also seen in SCA23 (80%) and SCA35 (89%). However, patients with SCA36 did not show the decreased vibration or position sense that was seen in 60% of patients with SCA23. Similarly, spasmodic torticollis, which is characteristically found in 44% of patients with SCA35, was not observed in patients with SCA36.

The lower motor involvement of the tongue and other systemic muscles found in SCA36 is a distinctive clinical feature that differentiates SCA36 from other types of dominant ataxias. In previous studies, tongue atrophy has been reported in 15% of SCA1 and 15% of SCA3 cases, and tongue fasciculation in 20% of SCA1 and 35% of SCA3 cases.[13–15] Tongue atrophy has not been reported in other types of SCA. We found tongue atrophy or fasciculation to be common in SCA36 (71%, table). In spite of prominent tongue atrophy in some patients, their swallowing

function was generally well-preserved (table), and oral intake continued even in the patients with disease duration of more than 20 years. The functionally benign tongue atrophy and the skeletal muscle atrophy in the limbs and trunk observed in SCA36 are similar to the disease manifestations seen in X-linked spinal and bulbar muscular atrophy.[16,17]

The overall clinical presentation, electrophysiologic, neuroradiologic, and neuropathologic findings of the 14 patients summarized here indicate that SCA36 is a relatively pure cerebellar ataxia with characteristic motor neuron involvement, which is especially prominent in the tongue. Further investigations of the SCA36 (GGCCTG)n expansion mutation will provide new insights into the pathogenic mechanisms involved in SCAs caused by noncoding microsatellite repeat expansions/insertions and will also shed light on other motor neuron diseases, including ALS.

AUTHOR CONTRIBUTIONS

Dr. Ikeda: drafting/revising the manuscript, study concept and design, analysis and interpretation of data, acquisition of data, statistical analysis, study supervision. Dr. Ohta: drafting/revising the manuscript, study concept and design, analysis and interpretation of data, acquisition of data. Dr. Kobayashi: drafting/revising the manuscript, study concept and design, analysis and interpretation of data, acquisition of data. Dr. M. Okamoto: drafting/revising the manuscript, study concept and design, analysis and interpretation of data, acquisition of data. Dr. Takamatsu: drafting/revising the manuscript, study concept and design, analysis and interpretation of data, acquisition of data. Dr. Ota: drafting/revising the manuscript, study concept and design, analysis and interpretation of data, acquisition of data. Dr. Manabe: drafting/revising the manuscript, study concept and design, analysis and interpretation of data, acquisition of data. Dr. K. Okamoto: drafting/revising the manuscript, study concept and design, analysis and interpretation of data, acquisition of data. Dr. Koizumi: drafting/revising the manuscript, study concept and design, analysis and interpretation of data, acquisition of data. Dr. Abe: drafting/revising the manuscript, study concept and design, analysis and interpretation of data, acquisition of data, study supervision.

ACKNOWLEDGMENT

The authors thank the patients and doctors who participated in this work.

DISCLOSURE

The authors report no disclosures relevant to the manuscript. **Go to Neurology.org for full disclosures.**

Received August 13, 2011. Accepted in final form December 8, 2011.

REFERENCES

1. Durr A. Autosomal dominant cerebellar ataxias: polyglutamine expansions and beyond. Lancet Neurol 2010;9:885–894.
2. Kobayashi H, Abe K, Matsuura T, et al. Expansion of intronic GGCCTG hexanucleotide repeat in NOP56 causes SCA36, a type of spinocerebellar ataxia accompanied by motor neuron involvement. Am J Hum Genet 2011;89:121–130.
3. Ikeda Y, Nagai M, Kurata T, et al. Comparisons of acoustic function in SCA31 and other forms of ataxias. Neurol Res 2011;33:427–432.
4. Ikeda Y, Shizuka M, Watanabe M, Okamoto K, Shoji M. Molecular and clinical analyses of spinocerebellar ataxia type 8 in Japan. Neurology 2000;54:950–955.
5. Waragai M, Yamada T, Matsuda H. Evaluation of brain perfusion SPECT using an easy Z-score imaging system (eZIS) as an adjunct to early diagnosis of neurodegenerative diseases. J Neurol Sci 2007;260:57–64.
6. Verbeek DS. Spinocerebellar ataxia type 23: a genetic update. Cerebellum 2009;8:104–107.
7. Verbeek DS, van de Warrenburg BP, Wesseling P, Pearson PL, Kremer HP, Sinke RJ. Mapping of the SCA23 locus involved in autosomal dominant cerebellar ataxia to chromosome region 20p13-12.3. Brain 2004;127:2551–2557.
8. Bakalkin G, Watanabe H, Jezierska J, et al. Prodynorphin mutations cause the neurodegenerative disorder spinocerebellar ataxia type 23. Am J Hum Genet 2010;87:593–603.
9. Wang JL, Yang X, Xia K, et al. TGM6 identified as a novel causative gene of spinocerebellar ataxias using exome sequencing. Brain 2010;133:3510–3518.
10. Ohta Y, Hayashi T, Nagai M, et al. Two cases of spinocerebellar ataxia accompanied by involvement of the skeletal motor neuron system and bulbar palsy. Intern Med 2007;46:751–755.
11. Fujita Y, Mizuno Y, Takatama M, Okamoto K. Anterior horn cells with abnormal TDP-43 immunoreactivities show fragmentation of the Golgi apparatus in ALS. J Neurol Sci 2008;269:30–34.
12. Elden AC, Kim HJ, Hart MP, et al. Ataxin-2 intermediate-length polyglutamine expansions are associated with increased risk for ALS. Nature 2010;466:1069–1075.
13. Watanabe M, Abe K, Aoki M, et al. Analysis of CAG trinucleotide expansion associated with Machado-Joseph disease. J Neurol Sci 1996;136:101–107.
14. Kameya T, Abe K, Aoki M, et al. Analysis of spinocerebellar ataxia type 1 (SCA1)-related CAG trinucleotide expansion in Japan. Neurology 1995;45:1587–1594.
15. Goldfarb LG, Vasconcelos O, Platonov FA, et al. Unstable triplet repeat and phenotypic variability of spinocerebellar ataxia type 1. Ann Neurol 1996;39:500–506.
16. La Spada AR, Wilson EM, Lubahn DB, Harding AE, Fischbeck KH. Androgen receptor gene mutations in X-linked spinal and bulbar muscular atrophy. Nature 1991;352:77–79.
17. Chahin N, Klein C, Mandrekar J, Sorenson E. Natural history of spinal-bulbar muscular atrophy. Neurology 2008;70:1967–1971.

Environ Health Prev Med (2013) 18:121–129
DOI 10.1007/s12199-012-0299-1

REGULAR ARTICLE

P.R4810K, a polymorphism of *RNF213*, the susceptibility gene for moyamoya disease, is associated with blood pressure

Akio Koizumi · Hatasu Kobayashi · Wanyang Liu · Yukiko Fujii · S. T. M. L. D. Senevirathna · Shanika Nanayakkara · Hiroko Okuda · Toshiaki Hitomi · Kouji H. Harada · Katsunobu Takenaka · Takao Watanabe · Shinichiro Shimbo

Received: 20 June 2012 / Accepted: 26 July 2012 / Published online: 10 August 2012

Abstract

Background Moyamoya disease—an idiopathic vascular disorder of intracranial arteries—is often accompanied by hypertension. *RNF213* has been identified as a susceptibility gene for moyamoya disease. In the present study, the association of p.R4810K (G>A) with blood pressure (BP) was investigated in a Japanese population.

Methodology/principal findings Three independent study populations, the Nyukawa ($n = 984$), Noshiro ($n = 2,443$) and Field ($n = 881$) studies, joined this study. BP, body weight and height were measured. Past and present symptoms and disease and medication histories were assessed by interview. Associations of p.R4810K (rs112735431, ss179362673) of *RNF213* with BP were investigated. Two linkage disequilibrium blocks were constructed for moyamoya patients with p.R4810K ($n = 140$) and the general population ($n = 384$) using 39 single nucleotide polymorphisms (SNPs) spanning 390 kb around *RNF213*. A total of 60 carriers (3 for AA genotype and 57 for GA genotype) were found in these samples, and the minor allele frequencies were 1.4 % in the Nyukawa and Field studies and 0.2 % in the Noshiro study. Regression analyses adjusted for age, sex and body mass index based on an additive model demonstrated significant associations with systolic BP (mmHg/allele): β (standard error) was 8.2 (2.9) in the Nyukawa study ($P = 4.7 \times 10^{-3}$), 18.7 (5.4) in the Noshiro study ($P = 4.6 \times 10^{-4}$) and 8.9 (2.0) ($P = 1.0 \times 10^{-5}$) in the three populations. In contrast, diastolic BP showed significant associations only in the Noshiro study. Linkage disequilibrium blocks contained none of the BP-associated proxy SNPs reported by previous studies.

Conclusions/significance Our study suggests that p.R4810K of *RNF213* is associated strongly with systolic BP.

Keywords *RNF213* · Moyamoya disease · P.R4810K · Systolic blood pressure · Hypertension

Electronic supplementary material The online version of this article (doi:10.1007/s12199-012-0299-1) contains supplementary material, which is available to authorized users.

A. Koizumi (✉) · H. Kobayashi · W. Liu · Y. Fujii · S. T. M. L. D. Senevirathna · S. Nanayakkara · H. Okuda · T. Hitomi · K. H. Harada
Department of Health and Environmental Sciences, Graduate School of Medicine, Kyoto University, Konoe-cho, Yoshida, Sakyo-ku, Kyoto 606-8501, Japan
e-mail: koizumi.akio.5v@kyoto-u.ac.jp

K. Takenaka
Department of Neurosurgery, Takayama Red Cross Hospital, Takayama, Japan

T. Watanabe
Department of Education, Tohoku Bunkyo College, Yamagata, Japan

S. Shimbo
Department of Food and Nutrition, Kyoto Women's University, Kyoto, Japan

Introduction

Moyamoya disease is an idiopathic occlusive vascular lesion that occurs at the terminal portion of internal carotid arteries in the circle of Willis [1, 2]. Familial clustering has been reported for moyamoya disease, with 15 % of cases being reported to have a family history [3]. This familial clustering led to searches for genetic factors, which identified several loci, including 3p24–p26 [4], 6q25 [5], 8q23 [6] and 17q25 [7, 8]. The locus on 17q25.3 was further refined by a linkage analysis [9] and an association study

[10]. Finally, *RNF213* was identified as the susceptibility gene of the 17q25.3 locus for moyamoya disease [11].

Several polymorphisms specific to Japanese, Korean, Chinese and Caucasian patients with moyamoya disease have been found in *RNF213* [11]. Of these, the p.R4810K (rs 112735431, ss179362673; G>A) polymorphism is a founder variant found commonly in Japanese, Korean and Chinese patients. In particular, it is found at rates of >90 % in Japanese patients and approximately 80 % in Korean patients. More surprisingly, 2–3 % of the Japanese and Korean general populations are carriers of this variant [11]. Given that the prevalence of moyamoya disease in patients is 10.5 per 10^5 people [12] and the rate of carriers of p.R4810K is 3 %, only a minor portion of carriers will develop moyamoya disease.

We conducted molecular cloning of a full-length cDNA of *RNF213* and found that it comprises 5,207 amino acids. *RNF213* has two well-known domains, a RING finger domain and a Walker motif that show ubiquitin ligase activity and ATPase activity, respectively [11]. *RNF213* was shown to be a novel functional E3 ligase [11]. Two splicing variants of *RNF213* were detected ubiquitously in cDNAs isolated from various types of cells, including vascular endothelial cells [11]. After knockdown of *RNF213* in zebrafish embryos, severely abnormal sprouting vessels were seen in the cranial vessels. However, the p.R4810K variant had no apparent detrimental effects on E3 ligase activity.

Moyamoya disease is often accompanied by hypertension [13, 14]. The pathogenesis of hypertension in patients with moyamoya disease has been attributed to stenosis of the renal arteries, i.e., renovascular hypertension. However, in some cases, hypertension was reported to occur without stenosis of the renal arteries [15]. Such observations suggest that hypertension in moyamoya disease may be caused by a novel mechanism associated with *RNF213* variants. If this is the case, it can be hypothesized that hypertension is a phenotype of p.R4810K carriers.

In the present study, we investigated whether p.R4810K elevates blood pressure (BP) in p.R4810K carriers. To examine this possibility, we conducted a genetic epidemiological study in three independent populations.

Methods

Ethical statement

Ethical approval for the three independent studies was given by the Institutional Review Board and Ethics Committee of Kyoto University School of Medicine, Kyoto University, Japan (Approval number: G140 approval date 10/18/2004). All the subjects provided written informed consent. All the studies involved the use of humans and adhered to the principles of the Declaration of Helsinki and Title 45, US Code of Federal Regulations, Part 46, Protection of Human Subjects.

Study population

Hypertension was defined as systolic blood pressure (SBP) of ≥140 mmHg and/or diastolic blood pressure (DBP) of ≥90 mmHg or treatment with antihypertensive medication. The pulse pressure (PP) was calculated as the difference between SBP and DBP.

Samples were donated by participants in three independent studies: the Nyukawa, Noshiro and Field studies. The Nyukawa and Noshiro studies are cohort studies to investigate common diseases. An annual health check-up is provided to the residents as a subsidy program run by the local autonomy at its public health center under the Industrial Safety and Health Act or Elderly Health law. Weight was measured in light clothes on an electrical balance, and height was measured with a stadiometer. Body mass index (BMI) was computed as weight in kilograms divided by the square of the height in meters. BP was measured on the right arm of seated participants by public health nurses after 5 min of rest at each examination using a mercury sphygmomanometer. BP was measured once or more than once when the readings were much higher than past records, i.e., 10 mmHg for SBP and 5 mmHg for DBP. In cases with more than one reading, the later BP reading was used. Clinical data such as past history of medication, past disease history, past and present symptoms, and demographic data (age and birth date) were collected by interview by public health nurses during the clinical examinations. The Nyukawa study started in 2004 in Nyukawa town in Gifu prefecture and has continued to the present, while the Noshiro study started in 1998 in Noshiro city in Akita prefecture and has continued to the present. All participants who underwent health check-ups at local health centers were recruited, and >95 % of the potential candidates agreed to join the present study. The participants donated blood samples at start of the studies and data collected at the start of the studies were used. Although these two studies are cohort studies, the study design for the present study was a cross-sectional association.

The Field study started in the early 1990s and ended in the mid-1990s as an environmental and nutritional study designed to evaluate exposure to environmental pollutants through dietary routes in nationwide general populations [16, 17]. Participants were recruited from among farmers by local community farming support stations. More than 90 % of subjects agreed to join the study. Owing to its focus on household information, such as dietary habits and

sources of vegetables, we selectively recruited more unrelated housewives than males. The researchers visited local towns and collected blood samples. Weight was measured in light clothes on a scale and height was measured with a stadiometer. BP was measured on the right arm of seated participants by physicians after 5 min of rest at each examination using a mercury sphygmomanometer. BP readings were measured once, and more than once when readings were much higher (i.e., 10 mmHg for SBP and 5 mmHg for DBP) than the values anticipated by the participants. In cases with more than one reading, the later BP reading was used. Clinical data such as past history of medication, past disease history, past and present symptoms, and demographic data (age and birth date) were collected by interview by physicians during the participant's visit. The samples and data were donated to the Kyoto Specimen sample bank [18, 19]. Since the minor allele frequency (MAF) of p.R4810K in the general population was significantly lower for the Noshiro population (0.2 %) than for the Nyukawa population (1.4 %), we selected populations in the western part of Japan in the Field study, i.e., Niigata, Ishikawa, Toyama, Tokyo, Gunma, Nagano, Aichi, Shiga, Kyoto, Kochi, Ehime, Shimane, Yamaguchi and Kagoshima.

We excluded from the analyses subjects with chronic kidney disease, polycystic kidney diseases, diabetic nephropathy and secondary hypertension based on the information obtained by interview. Blood-relatedness of the participants was checked by address, family names and interviews. If there was blood-relatedness among participants, one of the blood-related participants was selected and others were excluded from the analyses. For carriers, interview sheets describing blood-relatedness among carriers within the same communities were re-reviewed. Carriers or related family members were re-interviewed if needed.

Linkage disequilibrium around ss179362673

In the Japanese population, haplotypes carrying p.R4810K in *RNF213* were reported to be derived from a common founder [11]. We investigated linkage disequilibrium (LD) blocks in unrelated Japanese controls ($n = 384$) in the Kyoto and Osaka areas in western Japan, and in Japanese patients with p.R4810K and moyamoya disease ($n = 140$) [11]. Thirty-two single nucleotide polymorphisms (SNPs) (rs6565649, rs7216577, rs7406843, rs8078855, rs7217421, rs9902702, rs11869363, rs12451808, rs55996424, rs7222014, rs35968416, rs4890012, rs12150356, rs8070106, rs4889848, rs6565683, rs9913006, rs6565686, rs8065843, rs4074303, rs4890025, rs11869626, rs9898443, rs12601738, rs12185227, rs7502866, rs9911978, rs12950635 rs4890047, rs4889863, rs11655474, rs8080957) were selected on the basis of information in the Hapmap database (http://hapmap.ncbi.nlm.nih.gov/) to cover a region spanning 390 kb from the 5′ end of *SGSH* to the 5′ end of *Raptor*. These 32 SNPs were selected to illustrate the LD blocks using the Tagger program, with criteria of $r^2 > 0.65$ and a MAF of >0.05 in Japanese people. Typing for these 32 SNPs plus 7 rare SNPs (ss179362670, ss179362671, ss179362672, ss179362673, ss179362674, ss179362675, ss161110142) was selected. Each LD block was constructed using SNP & Variation Suite V7. LDs were evaluated by D'.

Genotyping and quality control

Genomic DNA was extracted from blood samples with a QIAamp DNA Blood Mini Kit (Qiagen, Tokyo, Japan). Genotyping of the 39 SNPs was conducted using TaqMan probes (TaqMan SNP Genotyping Assays; Applied Biosystems, Tokyo, Japan) using a 7300/7500 Real-Time PCR System (Applied Biosystems, Foster City, CA) as previously reported [11]. Data were cleaned using a quality control process. This process included evaluation of sample and marker call rates, mismatches of sex, age and BP readings, past histories, duplicates and batch effects. Sample relatedness and population stratification were not evaluated genetically. The genotyping results for p.R4810K were confirmed by direct sequencing by the Sanger method in 42 subjects out of 140 patients, as previously reported [11]. The genotype of p.R4810K in two independent genotyping procedures was perfectly matched for control 384 subjects. The call rates for the 39 SNPs were 100 %.

Statistical analysis

Hypertension was analyzed as a binary trait (cases vs controls) using a logistic model under an additive model. Association of p.R4810K with BP was also analyzed by an additive model as a quantitative trait using linear regression models. For subjects taking antihypertensive therapies, BPs were imputed by adding 10 and 5 mmHg to the SBP and DBP values, respectively [20]. Unless otherwise specified, analyses were based on the protocol used in the large studies [21–23]: adjustment for age, sex and BMI: inclusion of subjects taking antihypertensive medications and imputation of their BP. Genetic association analyses were performed using SNP & Variation Suite V7 (Golden Helix, Bozeman, MT). In the analyses, we tested additive and dominant models. Odds ratio was calculated by the SNP & Variation Suite for dichotomous phenotypes. Hardy-Weinberg equilibrium (HWE) was tested in entire populations. The exclusion criteria was HWE $<10^{-3}$.

A Bonferroni correction of $P = 0.05/2 = 0.025$ was applied to the regression analysis. This correction was selected because two parameters, SBP and DBP, were independent, while the other parameters (PP and adjusted

values) were derivatives of these values. Other statistical analyses were conducted using SAS software (SAS Institute, Cary, NC). A value of $P < 0.05$ was considered to indicate statistical significance.

Results

Demographic characteristics of three populations

The demographic characteristics of the participants in the three studies are summarized in Table 1. The numbers of participants were 984 for the Nyukawa study, 2,443 for the Noshiro study and 881 for the Field study. The percentages of patients taking antihypertensive agents or diuretics ranged from 10.8 % in the Field study to 15.8 % in the Noshiro study. The percentages of patients with hypertension ranged from 12.8 % in the Field study to 17.6 % in the Noshiro study.

The MAFs of p.R4810K were 1.4 % in the Nyukawa and Field studies, and 0.2 % in the Noshiro study (Table 2). The MAF was significantly lower in the Noshiro study than in the Nyukawa and Field studies (Fisher's exact test, $P < 1 \times 10^{-5}$). Based on interview, none of the carriers had any symptoms related to moyamoya disease or past history of stroke.

Blood-relatedness checked by address and family names did not exclude any subjects in three studies. None of the 60 carriers were confirmed to be blood-related by re-review of the interview sheets.

Table 1 Demographic characteristics of the three samples

Characteristics	Nyukawa study	Noshiro study	Field study
Observation period	2004-present	1998-present	1990s
Number of participants	984	2,443	881
Men:women	425:559	1,229:1,214	188:693
Age (years)	56.1 ± 15.1	49.9 ± 14.0	50.8 ± 10.4
Body mass index (BMI)	22.3 ± 2.9	23.3 ± 3.1	23.2 ± 3.0
SBP (mmHg)	125.2 ± 19.2	126.6 ± 18.2	129.1 ± 13.8
DBP (mmHg)	72.7 ± 12.1	77.5 ± 11.9	76.6 ± 10.3
% Taking antihypertensive or diuretics	10.9	15.8	10.8
% Hypertension	15.5	17.6	12.8

Data are shown as values or mean ± standard deviation (SD)

Table 2 Association of p.R4810K with hypertension by additive model

Study	p.R4810K genotype (G>A)						Dichotomous	
	AA	GA	GG	Total	MAF (%)		HT (+)	HT (−)
Nyukawa	2	23	959	984	1.4	AA	1	1
						AG	6	17
						GG	145	814
						Odds (95 % CI)	2.09 (0.96–4.58)	
	HWE	0.012				*P*	0.08	
Noshiro	0	11	2,432	2,443	0.2	AG	3	8
						GG	428	2004
						Odds (95 % CI)	1.76 (0.46–6.64)	
	HWE	1				*P*	0.368	
Field	1	23	857	881	1.4	AA	0	1
						AG	5	18
						GG	108	749
						Odds (95 % CI)	1.93 (0.70–5.30)	
	HWE	0.159				*P*	0.329	
Combined	3	57	4,248	4,308	0.7	AA	1	2
						AG	14	43
						GG	681	3567
						Odds (95 % CI)	1.71 (0.93–3.13)	
	HWE	1.39×10^{-3}				*P*	0.055	

MAF minor allele frequency, *HT* hypertension, *CI* confidence interval, *HWE* Hardy–Weinberg equilibrium

Table 3 Association of p.R4810K with blood pressures by additive model and dominant model

	SBP			DBP			PP		
	β	SE	p	β	SE	p	β	SE	p
Additive model study									
	Raw data (mm Hg)								
Nyukawa	8.2	2.9	$4.7 \times 10^{-3*}$	−0.4	2.0	0.83	8.5	2.1	$4.6 \times 10^{-5*}$
Noshiro	18.7	5.4	$4.6 \times 10^{-4*}$	11.4	3.4	$6.6 \times 10^{-4*}$	7.3	2.8	$1.0 \times 10^{-2*}$
Field studies	4.7	2.4	5.6×10^{-2}	−0.4	2.0	0.83	5.1	2.2	$1.8 \times 10^{-2*}$
Combined	8.9	2.0	$1.0 \times 10^{-5*}$	0.6	1.9	0.70	8.3	1.3	$5.4 \times 10^{-11*}$
	Adjusted data (mmHg)								
Nyukawa	10.0	3.2	$1.6 \times 10^{-3*}$	0.5	2.1	0.82	9.6	2.2	$1.7 \times 10^{-5*}$
Noshiro	19.1	5.8	$1.0 \times 10^{-3*}$	11.6	3.6	$1.2 \times 10^{-3*}$	7.5	3.0	$1.4 \times 10^{-2*}$
Field studies	6.1	2.6	$2.0 \times 10^{-2*}$	0.3	2.0	0.88	5.8	2.2	$8.6 \times 10^{-3*}$
Combined	10.0	2.2	$5.0 \times 10^{-5*}$	1.2	1.4	0.40	8.9	1.3	$2.3 \times 10^{-11*}$
Dominant model study									
	Raw data (mm Hg)								
Nyukawa	9.2	3.2	$4.4 \times 10^{-3*}$	−0.2	2.2	0.94	9.4	2.4	$7.6 \times 10^{-5*}$
Noshiro	18.7	5.4	$4.6 \times 10^{-4*}$	11.4	3.4	$6.6 \times 10^{-4*}$	7.3	2.8	$1.0 \times 10^{-2*}$
Field studies	6.3	1.7	$3.0 \times 10^{-4*}$	0.04	1.4	0.97	6.2	1.5	$3.1 \times 10^{-5*}$
Combined	9.9	2.2	$5.7 \times 10^{-6*}$	1.1	1.5	0.46	8.8	1.4	$1.0 \times 10^{-10*}$
	Adjusted data (mmHg)								
Nyukawa	10.8	3.5	$2.3 \times 10^{-3*}$	0.6	2.3	0.78	10.2	2.5	$4.0 \times 10^{-5*}$
Noshiro	19.1	5.8	$1.0 \times 10^{-3*}$	11.6	3.6	$1.2 \times 10^{-3*}$	7.5	3.0	$1.4 \times 10^{-2*}$
Field studies	6.7	2.8	$2.0 \times 10^{-2*}$	0.5	2.2	0.82	6.9	2.5	$5.4 \times 10^{-3*}$
Combined	10.8	2.4	$4.9 \times 10^{-6*}$	1.5	1.5	0.92	9.2	1.4	$8.5 \times 10^{-11*}$

* Significant association $p < 0.025$

Association of p.R4810K with hypertension

The associations of p.R4810K by the additive model for dichotomous traits (hypertension vs normal) were not significant in any of the populations (Table 2).

Regression analyses adjusted for age, sex and BMI revealed significant associations of p.R4810K with SBP and PP (Table 3). Specifically, the β [standard error (SE)] values for SBP were 8.2 (2.9) mmHg/allele for the Nyukawa study and 18.7 (5.4) mmHg/allele for the Noshiro study, while those for PP were 8.5 (2.1) mmHg/allele for the Nyukawa study, 7.3 (2.8) mmHg/allele for the Noshiro study and 5.1 (2.2) mmHg/allele for the Field study. The associations of p.R4810K with therapy-adjusted SBP and PP were also confirmed in the three studies. In the three combined populations, p.R4810K was highly associated with SBP [8.9 (2.0) mmHg/allele] and adjusted SBP [10.0 (2.2) mmHg/allele]; with PP [8.3 (1.3) mmHg/allele] and adjusted PP [8.9 (1.3) mmHg/allele]. The results by additive model are essentially the same by dominant model.

The characteristic features of carriers are shown in Table 4. SBP was significantly higher for the AA + GA genotype than for the GG genotype [136.4 (20.3) vs 126.4 (18.2) mmHg/allele, $P < 0.001$], while the male/female ratios, age and BMI did not differ significantly between any two groups. Adjusted SBP (mmHg/allele: mean ± SD) was 155.3 (19.7) for the AA genotype, 137.8 (22.7) for the GA genotype and 138.7 (22.7) for the AA + GA genotype, which is significantly higher than 127.7 (19.9) with the GG genotype ($P < 0.001$). On the other hand, neither DBP nor adjusted DBP differed between any two groups: the adjusted BP was 78.2 (13.2) and 76.9 (12.5) for GG genotypes, respectively. The % hypertension was marginally higher in the AA + AG group than in the GG group (Fisher's exact test, $P = 0.06$).

Effects on associations of protocol changes for statistical analysis

The present statistical analyses were based on the same protocol [21–23]. The protocol included subjects with antihypertensive medications and adjustment for age, sex and BMI. We investigate the effects of modifications of the protocol on the statistical analyses to determine to what degree the current results are dependent on the protocol. First, we eliminated subjects with antihypertensive

Table 4 Characteristics of p.R4810K carriers. Values are mean (standard deviation)

Genotype	*N*	M:F	Age (years)	BMI	Raw blood pressure (mmHg)		% Hypertension
					SBP	DBP	
AA	3	1:2	72.7 (5.1)	23.2 (4.8)	145.3 (19.7)	73.3 (5.8)	66.7
GA	57	14:43	51.9 (21.4)	23.5 (3.9)	135.9 (20.4)	77.3 (13.1)	24.6
AA + GA	60	15:45	52.4 (14.0)	23.5 (3.9)	136.4 (20.3)*	77.1 (12.8)	25.0
GG	4,248	1,827:2,421	51.1 (13.9)	23.0 (3.0)	126.4 (18.2)	76.2 (11.8)	16.0

* Significantly different from the values in GG genotype $P < 0.001$

medications to investigate the effect of genotypes without modifications by medications. Although reduced numbers of subjects decreased statistical power, there were significant associations of p.R4810K with SBP and PP (Table S1). Second, analyses were conducted without adjustment for BMI for the population including subjects with antihypertensive medications. The associations were reproduced without adjustment for BMI (Tables S2 and S3). Changes in the statistical analysis protocol did not alter the results by quantitative regression analyses extensively, suggesting that associations of p.R4810K are robust and reproducible.

LD blocks around p.R4810K of *RNF213*

Analyses of the LD blocks of 39 SNPs spanning 390 kb in patients with p.R4810K and moyamoya disease demonstrated that p.R4810K was in LD with the 3′ half of *RNF213* and *ENDOV* (Fig. 1a). Similar LD blocks were observed in the general control population (Fig. 1b). LD blocks of p.R4810K did not contain any proxy SNPs, which have been reported to be associated with BP in East Asian people or other ethnicities, even when less stringent statistical criteria are applied [21–23].

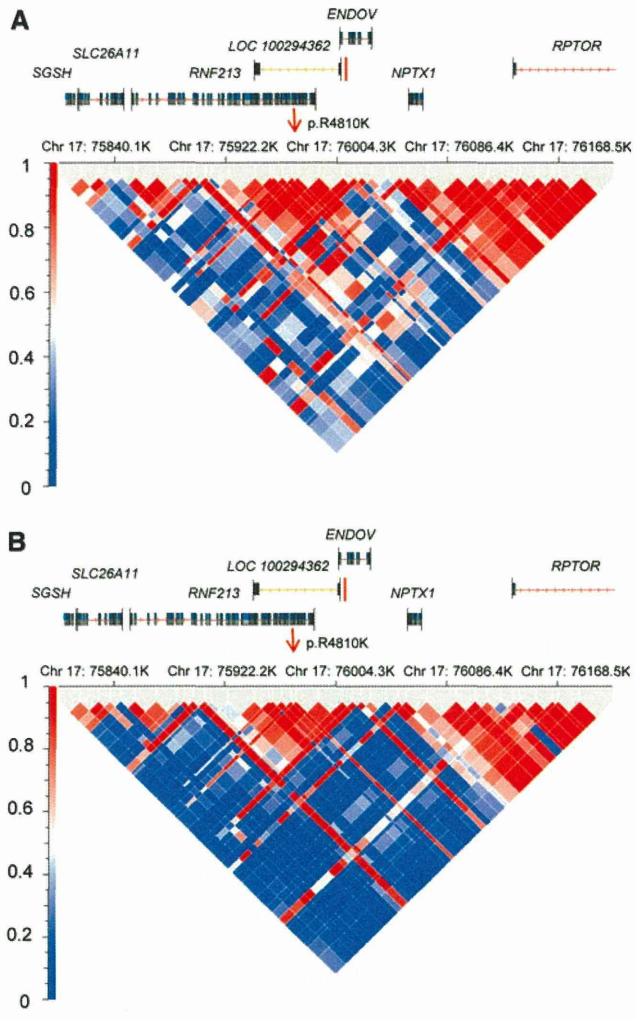

Fig. 1 Linkage disequilibrium (LD) blocks from a region spanning 390 kb from *SGSH* to *RAPTOR* in two independent populations. The LD blocks were constructed with 39 single nucleotide polymorphisms (SNPs). Scales are *D′*. The physical positions refer to Genome View Build 36 (http://www.ncbi.nlm.nih.gov/mapview/). **a** LD blocks for 140 unrelated Japanese patients with p.R4810K and moyamoya disease. **b** LD blocks for 384 unrelated Japanese subjects

Discussion

In the present study, quantitative trait locus analyses demonstrated that p.R4810K was associated significantly with SBP and PP in the general population. The p.R4810K allele resulted in consistently elevated SBP from 4.7 to 18.7 mmHg/allele and PP from 5.1 to 8.5 mmHg/allele. Such large and consistent contributions support our hypothesis that p.R4810K increases SBP.

Several large-scale studies have used the genome-wide association study (GWAS) approach [21–23]. However, none of these studies detected a locus on 17q25.3 for hypertension. Investigations of the LD blocks of p.R4810K failed to reveal any SNPs that have been reported to be associated with BP, even with less stringent *P* values [21–23]. There is no doubt that recent association studies have been successful; however, we consider that there are three major reasons for the failure to detect an association of *RNF213* polymorphisms with hypertension. First, the

critical assumption for the efficient detection of association through GWAS using LD mapping with TagSNPs ≥5 % is that, for the susceptibility locus, there is only low level allelic heterogeneity. In the presence of allelic heterogeneities, GWAS with TagSNPs may have missed potentially significant associations [24, 25]. Second, another GWAS assumption is that variants are common. The GWAS protocol usually discards minor alleles, i.e., with allele frequencies smaller than 10 %. Thus, minor alleles in *RNF213*, such as p.R4810K, might have been eliminated from the analysis. Third, even large studies are not free from sample size limitations to detect small population effects even using TagSNPs. For example, a simple genetic power calculation [26] on the assumption (HT prevalence 0.2; risk of the allele = 2.0; D' between a tag SNP and risk allele 0.9; tag SNP allele frequency = 0.5) reveals that to obtain alpha = 0.05 and power = 0.80, more than 50,000 HT Japanese cases would be needed for the low frequencies of risk allele ~0.01. Given the lower frequencies in the Tohoku areas of Japan, more cases would have been needed. Collectively, although p.R4810K has a discernible influence on BP in individuals, its small contribution to the population BP makes it extremely difficult to detect, even in large scale GWAS studies.

Given that the current observation can be generalized, carriers of p.R4810K are at risk of high SBP, irrespective of whether they have moyamoya disease. An increase of this magnitude overwhelms the population average of BP treatment effects for single antihypertensive agents [27]. Moreover, it has been suggested that differences in SBP of this magnitude elevate total mortality and the incidence of stroke [28]. Therefore, p.R4810K carriers may need special attention to control their SBP to prevent cerebrovascular events, regardless of whether they are affected by moyamoya disease. In this regard, it remains an enigma why p.R4810K has a strong association with SBP while it does not with DBP. Further studies are warranted to explain the preferential association with SBP.

Hypertension in patients with moyamoya disease has been postulated to be caused by renovascular hypertension [13, 14]. Similarly, it may occur in carriers without manifestation of moyamoya disease. There may also be other possibilities for the mechanisms of hypertension. For example, it remains to be addressed why hypertension occurs in some patients with moyamoya disease without stenosis of the renal arteries [15]. The physiological role of the p.R4810K variant of *RNF213* in the pathological process is unknown. *RNF213* comprises a novel class of E3 ligase and is involved in angiogenesis [11]. Therefore, its biochemical and physiological functions need to be elucidated. Further studies are required with a focus on the functional aspects of p.R4810K of *RNF213* in SBP.

Except for Down syndrome [29], various disorders associated with moyamoya syndrome are also known to be associated with BP, including Sickle cell disease [30, 31], neurofibromatosis I [32], Noonan syndrome [33, 34], Seckel syndrome [35], familial thoracic aortic aneurysm/dissection syndrome caused by *ACTA2* mutations [36] and X-linked moyamoya syndrome [37]. The genetic association between BP and p.R4810K of *RNF213* may not be unique to moyamoya disease, but could instead be common to the pathophysiology associated with moyamoya syndrome. The common pathological processes in these diseases are associated with occlusive vascular lesions. The biomedical mechanisms associated with occlusive vascular lesions may be attributable to endothelial dysfunction, as is the case for prehypertension [38]. Alternatively, it is interesting that patients with *ACTA2* mutations have excessive proliferation of vascular smooth muscle cells, and thereby elevated BP [36].

The present study has several limitations, the most major being the population sizes of the carriers of p.R4810K. Although we performed extensive genotyping in the three populations, we could not obtain large numbers of carriers because of the low prevalence of p.R4810K. It is of particular interest that the MAF of p.R4810K is significantly lower in the eastern part of mainland of Japan than in the western part of Japan. It should be investigated in future whether or not the prevalence of moyamoya disease has geographic differences in Japan. Specifically, it may be lower in the eastern part of mainland Japan than in the western part of Japan, as predicted by the low prevalence in Caucasians [11]. In this regard, although we cannot eliminate the effects of population stratification completely, the strength of the present study, namely a single ethnicity, can mitigate such biases. In addition, we did not test genetic relatedness among participants, although we checked it with indirect information. Thus, blood-related samples may be contaminated in associations and lead to inflation of associations. The second limitation of this study is that clinical data were not available for examining renovascular hypertension in carriers. Third, it could be argued p.R4810K is a proxy SNP or that *RNF213* is associated directly with BP, and that p.R4810K of *RNF213* may elevate BP. At present, we cannot say whether *RNF213* is associated with BP, and whether p.R4180K elevates BP directly or not. Further evidence is required to explain the association of p.R4810K with BP biologically. Finally, we cannot exclude a healthy participant effect in the current study. In fact, most of the participants are active both mentally and physically. Handicapped subjects with hypertension-associated cardiovascular diseases or subjects receiving clinical care might have been eliminated in the communities. The present findings may help to determine the pathological consequences of moyamoya disease in

carriers of p.R4810K. Furthermore, our findings suggest that high SBP may be a common phenotype of carriers of p.R4810K. Finally, although the MAF of p.R4810K in the general population is small, antihypertensive measures may be efficient for this high-risk population.

Acknowledgments We thank Dr. Kayoko Inoue, who died in 2007, Prof. Yasuhiko Wada (University of Kochi Prefecture) and Prof. Masayuki Ikeda (Kyoto Industrial Health Association). We are also grateful to Ms. Misato Umakosi (Kyoto University Graduate School of Medicine). This work was supported mainly by grants from the Ministry of Education, Culture, Sports, Science and Technology of Japan (Kiban Kenkyu A: 22249020) from the ministry of Health, Labour and Welfare of Japan (H23-Nanji-Ippan-019, chaired by Dr. Nobuo Hashimoto) and partially by a grant from Creative Scientific Research (19G50314).

Conflict of interest None.

References

1. Takeuchi K, Shimizu K. Hypogenesis of bilateral internal carotid arteries. Brain Nerve. 1957;9:37–43.
2. Suzuki J, Takaku A. Cerebrovascular "moyamoya" disease. Disease showing abnormal net-like vessels in base of brain. Arch Neurol. 1969;20:288–99.
3. Mineharu Y, Takenaka K, Yamakawa H, Inoue K, Ikeda H, et al. Inheritance pattern of familial moyamoya disease: autosomal dominant mode and genomic imprinting. J Neurol Neurosurg Psychiatry. 2006;77:1025–9.
4. Ikeda H, Sasaki T, Yoshimoto T, Fukui M, Arinami T. Mapping of a familial moyamoya disease gene to chromosome 3p24.2-p26. Am J Hum Genet. 1999;64:533–7.
5. Inoue TK, Ikezaki K, Sasazuki T, Matsushima T, Fukui M. Linkage analysis of moyamoya disease on chromosome 6. J Child Neurol. 2000;15:179–82.
6. Sakurai K, Horiuchi Y, Ikeda H, Ikezaki K, Yoshimoto T, et al. A novel susceptibility locus for moyamoya disease on chromosome 8q23. J Hum Genet. 2004;49:278–81.
7. Yamauchi T, Tada M, Houkin K, Tanaka T, Nakamura Y, et al. Linkage of familial moyamoya disease (spontaneous occlusion of the circle of Willis) to chromosome 17q25. Stroke. 2000;31: 930–5.
8. Mineharu Y, Liu W, Inoue K, Matsuura N, Inoue S, et al. Autosomal dominant moyamoya disease maps to chromosome 17q25.3. Neurology. 2008;70:2357–63.
9. Liu W, Hashikata H, Inoue K, Matsuura N, Mineharu Y, et al. A rare Asian founder polymorphism of Raptor may explain the high prevalence of moyamoya disease among East Asians and its low prevalence among Caucasians. Environ Health Prev Med. 2010; 15:94–104.
10. Kamada F, Aoki Y, Narisawa A, Abe Y, Komatsuzaki S, et al. A genome-wide association study identifies RNF213 as the first moyamoya disease gene. J Hum Genet. 2011;56:34–40.
11. Liu W, Morito D, Takashima S, Mineharu Y, Kobayashi H, et al. Identification of RNF213 as a susceptibility gene for moyamoya disease and its possible role in vascular development. PLoS ONE. 2011;6:e22542.
12. Kuroda S, Houkin K. Moyamoya disease: current concepts and future perspectives. Lancet Neurol. 2008;7:1056–66.
13. Yamada I, Himeno Y, Matsushima Y, Shibuya H. Renal artery lesions in patients with moyamoya disease: angiographic findings. Stroke. 2000;31:733–7.
14. Togao O, Mihara F, Yoshiura T, Tanaka A, Kuwabara Y, et al. Prevalence of stenoocclusive lesions in the renal and abdominal arteries in moyamoya disease. AJR Am J Roentgenol. 2004;183:119–22.
15. Limaye CS, Khude S, Pednekar SJ. Moyamoya disease with hypertension in a young adult. J Assoc Physicians India. 2011;59: 124–6.
16. Shimbo S, Zhang ZW, Moon CS, Watanabe T, Nakatsuka H, et al. Correlation between urine and blood concentrations, and dietary intake of cadmium and lead among women in the general population of Japan. Int Arch Occup Environ Health. 2000;73:163–70.
17. Watanabe T, Shimbo S, Nakatsuka H, Koizumi A, Higashikawa K, et al. Gender-related difference, geographical variation and time trend in dietary cadmium intake in Japan. Sci Total Environ. 2004;329:17–27.
18. Koizumi A, Yoshinaga T, Harada K, Inoue K, Morikawa A, et al. Assessment of human exposure to polychlorinated biphenyls and polybrominated diphenyl ethers in Japan using archived samples from the early 1980s and mid-1990s. Environ Res. 2005;99:31–9.
19. Koizumi A, Harada KH, Inoue K, Hitomi T, Yang HR, et al. Past, present, and future of environmental specimen banks. Environ Health Prev Med. 2009;14:307–18.
20. Cui JS, Hopper JL, Harrap SB. Antihypertensive treatments obscure familial contributions to blood pressure variation. Hypertension. 2003;41:207–10.
21. Levy D, Ehret GB, Rice K, Verwoert GC, Launer LJ, et al. Genome-wide association study of blood pressure and hypertension. Nat Genet. 2009;41:677–87.
22. Ehret GB, Munroe PB, Rice KM, Bochud M, Johnson AD, et al. Genetic variants in novel pathways influence blood pressure and cardiovascular disease risk. Nature. 2011;478:103–9.
23. Kato N, Takeuchi F, Tabara Y, Kelly TN, Go MJ, et al. Meta-analysis of genome-wide association studies identifies common variants associated with blood pressure variation in East Asians. Nat Genet. 2011;43:531–8.
24. Gorlov IP, Gorlova OY, Sunyaev SR, Spitz MR, Amon CI. Shifting paradigm of association studies: value of rare single nucleotide polymorphisms. Am J Human Genet. 2008;82:100–12.
25. Slager SL, Huang J, Vieland VJ. Effect of allelic heterogeneity on the power of the transmission disequilibrium test. Genet Epidemiol. 2000;18:143–56.
26. Purcell S, Cherny SS, Sham PC. Genetic power calculator: design of linkage and association genetic mapping studies of complex traits. Bioinformatics. 2003;19:149–50.
27. Burt VL, Cutler JA, Higgins M, Horan MJ, Labarthe D, et al. Trends in the prevalence, awareness, treatment, and control of hypertension in the adult US population. Data from the health examination surveys, 1960 to 1991. Hypertension. 1995;26:60–9.
28. Staessen JA, Gasowski J, Wang JG, Thijs L, Den Hond E, et al. Risks of untreated and treated isolated systolic hypertension in the elderly: meta-analysis of outcome trials. Lancet. 2000;355:865–72.
29. Draheim CC, Geijer JR, Dengel DR. Comparison of intima-media thickness of the carotid artery and cardiovascular disease risk factors in adults with versus without the Down syndrome. Am J Cardiol. 2010;106:1512–6.
30. Koduri PR, Agbemadzo B, Nathan S. Hemoglobin S-C disease revisited: clinical study of 106 adults. Am J Hematol. 2001;68:298–300.
31. Reid HL, Anah CO. Haemorheological parameters in hypertensive Nigerians with and without sickle-cell trait. Angiology. 1985;36:379–86.
32. Zinnamosca L, Petramala L, Cotesta D, Marinelli C, Schina M, et al. Neurofibromatosis type 1 (NF1) and pheochromocytoma: prevalence, clinical and cardiovascular aspects. Arch Dermatol Res. 2011;303:317–25.